DOI:
10.1038/s41419-020-2687-6

Document Version
Peer reviewed version

β-catenin promotes endothelial survival by regulating eNOS activity and flow-dependent anti-apoptotic gene expression

Virginia Tajadura[1], Marie Haugsten Hansen[1], Joy Smith[1], Hannah Charles[1], Matthew Rickman[2], Keith Farrell-Dillon[1], Vasco Claro[1], Christina Warboys[2,3*] and Albert Ferro[1*]

[1]School of Cardiovascular Medicine & Sciences, British Heart Foundation Centre of Research Excellence, King's College London, London SE1 9NH, UK
[2]Department of Bioengineering, Imperial College London, London, SW7 2BP, UK
[3]Department of Comparative Biomedical Sciences, Royal Veterinary College, London, NW1 0TU, UK

*Joint corresponding author

Running title: β-catenin and the anti-apoptotic effects of eNOS

Correspondence to:
Albert Ferro, School of Cardiovascular Medicine & Sciences, British Heart Foundation Centre of Research Excellence, King's College London, London SE1 9NH, UK
Phone: +44(0)20 7848 4283 E-mail: albert.ferro@kcl.ac.uk

OR

Christina Warboys, Department of Comparative Biomedical Sciences, Royal Veterinary College, London NW1 0TU, UK
Phone +44 (0)203 905 4790 E-mail cwarboys@rvc.ac.uk

Keywords: nitric oxide, β-catenin, gene transcription, disturbed flow, apoptosis

Word counts:

Abstract: 262
Main text (excluding abstract, materials & methods, references, figures & tables): 3,499

Number of figures and tables: 11 **(**6 figures, 1 table, 5 supplementary figures and 1 supplementary table).

Sources of support: This work was supported by a grant from the British Heart Foundation to AF and CW (PG/15/116/31947).

Abstract

Increased endothelial cell apoptosis is associated with the development of atherosclerotic plaques that develop predominantly at sites exposed to disturbed flow. Strategies to promote endothelial cell survival may therefore represent a novel therapeutic approach in cardiovascular disease. Nitric oxide (NO) and β-catenin have both been shown to promote cell survival and they interact in endothelial cells as we previously demonstrated. Here we investigated the physiological role of β-catenin as a mediator of NO-induced cell survival in endothelial cells. We found that β-catenin depleted human umbilical vein endothelial cells (HUVEC) stimulated with pharmacological activators of endothelial NO synthase (eNOS) showed a reduction in eNOS phosphorylation (Ser1177) as well as reduced intracellular cyclic guanosine monophosphate (cGMP) levels compared to control cells in static cultures. In addition, β-catenin depletion abrogated the protective effects of the NO donor, SNAP, during TNFα- and H_2O_2-induced apoptosis. Using an orbital shaker to generate shear stress, we confirmed eNOS and β-catenin interaction in HUVEC exposed to undisturbed flow (UF) and disturbed flow (DF) and showed that β-catenin depletion reduced eNOS phosphorylation. β-catenin depletion promoted apoptosis exclusively in HUVEC exposed to DF as did inhibition of soluble guanylate cyclase (sGC) or β-catenin transcriptional activity. The expression of the pro-survival genes, Bcl-2 and survivin was also reduced following inhibition of β-catenin transcriptional activity, as was the expression of eNOS. In conclusion, our data demonstrate that β-catenin is a positive regulator of eNOS activity and cell survival in human endothelial cells. sGC activity and β-catenin-dependent transcription of Bcl-2, survivin, BIRC3 and eNOS are essential to maintain cell survival in endothelial cells under DF.

Introduction

Apoptosis is implicated in a number of cardiovascular diseases, in particular the development and progression of atherosclerosis, plaque rupture, ischaemia reperfusion injury and heart failure[1]. Increased endothelial cell (EC) apoptosis is associated with the development of atherosclerotic plaques[2], vascular injury[3] and raised vessel permeability[4]. Strategies to promote cell survival may therefore be important in reducing cardiovascular disease.

Atherosclerosis is characterised by dysfunction of the vascular endothelium which is associated with reduced bioavailability and bioactivity of nitric oxide (NO)[5]. Endothelial NO synthase (eNOS), the main vascular source of NO, confers protection from cardiovascular disease[6], through a number of mechanisms including inhibition of EC apoptosis[7,8,9,10,11]. Similarly, laminar shear stress prevents TNFα and H_2O_2-induced apoptosis and this effect is dependent on eNOS activity[9]. NO has previously been shown to inhibit apoptosis at several levels; via S-nitrosylation of caspases[8,12], increased expression and stability of Bcl-2 by destabilization of MKP-3 mRNA[13] and inhibition of JNK signalling pathways[7,14]. Recently we identified β-catenin as a novel eNOS binding partner in human umbilical vein EC (HUVEC) and showed that pharmacological activation of eNOS, acting through sGC and cGMP, promotes nuclear translocation of β-catenin and transcription of some β-catenin target genes providing evidence of a novel signalling axis in EC[15].

β-catenin is a component of the adherens junction, linking VE-cadherin to the actin cytoskeleton, where it plays an important role in the dynamic regulation of endothelial permeability[16]. Non-junctional (cytosolic) β-catenin is rapidly degraded under resting conditions by interacting with an inhibitory complex comprised of APC, axin and GSK-3β that phosphorylates β-catenin and targets it for ubiquitin-mediated degradation[16]. Cytosolic β-catenin can be stabilised by canonical and non-canonical Wnt signalling pathways and, as recently established, by NO-cGMP signalling[15], whereby dephosphorylated (active) β-catenin

accumulates and translocates to the nucleus where it regulates gene expression through its interaction with TCF-LEF transcription factors[16]. A subset of β-catenin target genes are associated with anti-apoptotic (cell survival) functions raising the possibility that NO may promote cell survival through transcriptional activation of β-catenin.

Here we sought to assess the role of β-catenin in eNOS signalling and the physiological role of the NO-cGMP-β-catenin axis on apoptosis in EC under disturbed (atheroprone) or undisturbed (atheroprotective) flow.

Materials and methods

Cell culture, transfection and application of shear stress

HUVEC were purchased from Promocell as pools from several donors and cultured in Promocell Endothelial Cell Growth Medium (containing 2% FCS). Cells were cultured at 37°C and 5% CO_2 and confluent HUVEC at up to passage 6 were used for experiments. Human aortic endothelial cells (HAEC) from single donors were purchased from Promocell and cultured on fibronectin in Endothelial Growth Medium MV (Promocell). HAEC were used up to passage 6. Mouse pulmonary endothelial cells (MPEC) were cultured as previously described[15]. Culture media was supplemented with 100 U/ml penicillin and 100 µg/ml streptomycin. Antibiotic free media was used for the cell assays and added before application of flow (see below) and/or before a treatment was added. At least 3 different biologically independent cell batches were studied for each experiment.

RNA interference was performed using siRNA sequences specific for human target genes. Non-targeting scrambled sequences were used as a control. HUVEC were transfected with siRNAs (100nM) using Lipofectamine RNAiMAX (Invitrogen) in serum-free media (Optimem,

Invitrogen) without antibiotics. Medium was changed to growth medium 16 h after transfection. Scrambled control and β-catenin siRNA pool was purchased from Ambion and Santa Cruz respectively.

For assays in which application of flow was required, an orbital shaker was used. EC were seeded at passage 3-7 onto fibronectin-coated 6-well plates. Where experiments required immunostaining, EC were seeded onto fibronectin-coated glass-bottom plates (In vitro scientific). Once monolayers were confluent (after 24-48hrs), media was changed and the 6-well plates were placed onto an orbital rotating platform (Grant Instruments) housed inside the incubator and cultured for a further 72 h. The radius of orbit of the orbital shaker was 10 mm and the rotation rate was set to 150 rpm which caused swirling of the culture medium over the cell surface that creates distinct flow patterns at the centre and edge of the well; cells at the edge are exposed to undisturbed uniaxial flow (UF) whereas cells at the centre are exposed to disturbed, multidirectional flow (DF)[17].

For transfection of HUVEC for flow experiments, immediately prior to seeding into 6-well plates, HUVEC were transfected with 100nM MISSION® pre-designed and validated siRNA targeting β-catenin (Sigma) or 100 nM scrambled control (Ambion) by electroporation. Electroporation was carried out using a Neon™ Transfection System according to manufacturer's instructions. Cells were seeded at a density of $1x10^5$ cells per well and cultured under static conditions for ~6h to allow cells to adhere and become confluent before exposure to flow using the orbital shaker method. For analysis of protein expression, 3 wells were pooled for each flow condition. Knockdown of target proteins was confirmed by western blot for each experiment.

EC were exposed to disturbed or undisturbed flow for 72h using an orbital shaker (150rpm; Grant Instruments) housed inside the incubator[17,18]. At least 3 different biologically independent cell batches were studied for each experiment.

Cell lysis, fractionation and western blotting

Cells were lysed in ice-cold RIPA buffer (1% Triton-X 100, 1% sodium deoxycholate, 2.5 mmol/l ethylenediaminetetraacetic acid (EDTA), 100 mmol/l NaCl, 20mmol/l Tris-base; pH 7.4) supplemented with protease and phosphatase inhibitor cocktails (Roche). Lysates were incubated on ice for 45 min, then centrifuged for 10 min at 16,000g to separate soluble from insoluble fractions.

Cell surface and cytosolic extracts were separated from nuclear. Cells were scraped, washed with phosphate-buffered saline (pH 7.4), resuspended in hypotonic buffer (10 mM Hepes (pH 7.9), 1.5 mM MgCl2, 10 mM KCl, 0.2 mM phenylmethylsulfonyl fluoride, and 0.5 mM dithiothreitol), and allowed to swell on ice for 10 min. After that 1% NP40 was added and the cells were homogenized with a syringe and needle and vortexed for 2 min. The nuclei were separated by spinning at 3300g for 5 min at 4 °C. The supernatant was used as soluble cytoplasmic/membrane extract. The nuclear pellet was extracted in nuclear extraction buffer (20 mM Hepes (pH 7.9), 100mM NaCl, 1.5 mM MgCl2, 1% Triton, 1 mM EDTA, 1 mM EGTA, 10% glycerol, 0.5 % deoxycholate, 0.1% SDS with protease and phosphatase inhibitor cocktails (Roche)) for 30 min on ice and centrifuged at 12,000g for 30 min. The supernatant was used as a nuclear extract.

Soluble nuclear and cytoplasmic/membrane protein lysates were analysed by SDS-PAGE and immunoblotting. Bound antibodies were visualised with horseradish peroxidase-conjugated anti-IgG antibodies and enhanced chemiluminescence susbtrates (Thermo Scientific). Antibodies for western blotting were obtained from the following sources: anti cleaved caspase 3, total caspase 3, β-catenin, eNOS, eNOS phosphoS1177, Calnexin, cIAP1, TBP (Cell Signalling), β-catenin, active β-catenin, VE-cadherin, eNOS phosphoS635, eNOS phosphoS114 (BD Biosciences), NOS3, PDHX and GAPDH (Santa Cruz).

cGMP ELISA

Lysates were extracted by addition of 0.1 mol/L HCl supplemented with 1 mmol/L 3-isobutyl-1-methylxanthine. cGMP concentration was assessed following acetylation using Cyclic GMP EIA Kit (Cayman Chemicals) according to the manufacturer's instructions. Resulting cGMP concentrations were normalized to protein content per sample.

Immunostaining and confocal microscopy

HUVEC on fibronectin-coated glass plates (In vitro scientific IBL) were fixed with 4% paraformaldehyde solution for 20 min, permeabilized with 0.1% Triton X-100 in PBS for 5 min and blocked with 5% BSA in PBS for a further 30 min. Cells were incubated overnight at 4°C with anti-cleaved caspase 3 antibody (cell signalling), active β-catenin (BD biosciences) or VE-Cadherin (BD Biosciences) or active β-catenin (Millipore) and/or 4',6-diamidino-2-phenylindole (DAPI) to stain nuclei. Images were generated with a Nikon Spinning disk confocal microscope using a 20x objective and Nikon software. The percentage of cleaved caspase 3 positive cells was calculated in at least 16 randomly selected fields of view for each condition, covering approximately 2000-4000 cells to estimate the level of apoptosis.

En face staining of mouse aortas

All procedures were conducted in accordance with the Directive 2010/63/EU of the European Parliament on the protection of animals used for scientific purposes, as enforced by national legislation, the UK Animal (Scientific Procedures) Act 1986 (as amended), under authorisation of the UK Home Office (Project License No. 70-8934). Male, 8-week-old C57BL/6J mice were purchased from Charles River Laboratories (Harlow, UK), maintained on a 12-hour day/night cycle, and fed a standard breeding/maintenance chow ad libitum (RM3, Special Diets Services, UK) for two weeks prior to tissue harvest. Mice were terminally anaesthetised with an overdose of pentobarbitone (120 mg/kg i.p.) then perfused transcardially with an ice-cold 0.9% saline, 100 U/ml heparin solution, followed by ice-cold 4% paraformaldehyde (Parafix, Pioneer Research Chemicals Ltd, UK). Aortas were removed intact from the heart to the renal

bifurcation, further post-fixed in 4% paraformaldehyde at 4°C overnight, then micro-dissected under a stereomicroscope in 0.1 M phosphate buffered saline to produce en face preparations. Co-localization of eNOS (C-20; Santa Cruz) and β-catenin (BD biosciences) was visualised in EC from wild type C57BL/6 mice by *en face* staining of susceptible (inner curvature) or protected (outer curvature) regions of the aorta followed by laser scanning confocal microscopy. Nuclei were stained with DAPI.

Proximity ligation assay

Proximity ligation assays were carried out using a Duolink *In-Situ* Detection Kit as previously described[15]. HUVEC were cultured in 6-well plates until confluent and subjected to flow for 72 h using an orbital shaker. Following flow exposure, cells were fixed with 4% paraformaldehyde then permeabilized with 0.5% Triton®X-100. In situ proximity ligation assay (PLA) was carried out using rabbit anti-eNOS and mouse anti- β-catenin primary antibodies in combination with Duolink In Situ Red Detection Kit (Sigma). PLA was carried out according to the manufacturer's instructions. Afterwards cells were washed to eliminate excess of reagents and cells were counterstained with 4',6-diamidino-2-phenylindole (DAPI) and VE-Cadherin (BD Biosciences) to visualize cell junctions and nuclei respectively. Images were generated with a Nikon Spinning disk confocal microscope using a 20x objective and Nikon software NIS elements. PLA analysis was carried out on confocal images. Approximately 2000 cells from 4 independent experiments were quantified. The PLA signal intensity per cell was analysed using Image J and the particle analysis function on PLA images and cells numbers calculated using the same function on DAPI images. A mask for the cell edge was generated with the VE-cadherin image and imposed over the PLA image to measure signal inside and outside of the mask.

TUNEL assay

To detect DNA fragmentation in apoptotic cells, terminal transferase dUTP Nick End Labelling (TUNEL) was performed as previously described[19]. A Click-iT TUNEL Alexa Fluor 594 Imaging Assay was used following the manufacturer instructions (Life technologies). Briefly cells were fixed using 4% paraformaldehyde in PBS for 15 min and followed by a permeabilization step with 0.25% Triton®X-100 for 20 min. Cells were then treated with terminal deoxynucleotidyl transferase (TdT) for 60 minutes at 37°C to allow the incorporation of modified dUTPs at the 3'-OH ends of fragmented DNA, followed by a Click-iT® reaction for 30 min at 37°C to label ends with a fluorescent dye through click chemistry. Afterwards cells were washed gently to eliminate excess of reagents and cells were counterstained with 4',6-diamidino-2-phenylindole (DAPI) and VE-Cadherin (BD Biosciences) to visualize the cell edges and nuclei respectively. Images were generated with a Nikon Spinning disk confocal microscope using a 20x objective and Nikon software NIS elements. The percentage of TUNEL positive cells was calculated in 16 selected fields of view for each condition, covering approximately 2000-4000 cells to estimate the level of apoptosis.

RNA isolation and quantitative RT-PCR

RNA was isolated from cells using RNeasy Mini kits (Qiagen). Contaminating DNA was removed by on-column DNase digestion (Qiagen). cDNA was prepared using a High-Capacity Reverse Transcription Kit (Thermo Scientific). Quantitative real-time PCR (qPCR) was carried out with cDNA using SYBR green mastermix (Primer Design). GADPH was used as a reference gene. The qPCR oligonucleotide primers used for *eNOS* were: F: CATCTTCAGCCCCAAACGGA R: AGCGGATTGTAGCCTGGAAC; for *Survivin*: F: TGAGAACGAGCCAGACTTGG R: TGTTCCTCTATGGGGTCGTCA; for *KLF-2*: F: TGGGCATTTTTGGGCTACCT R: CCCAGTTCCAAGCAACCAGA; for *E-SEL*: F: GCTCTGCAGCTCGGACAT R: GAAAGTCCAGCTACCAAGGGAAT; for *Bcl-2*: F: ATGTGTGTGGAGAGCGTCAA R: GGGCCGTACAGTTCCACAAA; for *GAPDH*: F: CTATAAATTGAGCCCGCAGCC R: ACCAAATCCGTTGACTCCGA; for *XIAP*: F: AGTGTCTGGTAAGAACTACTG R: CCCATTCGTATAGCTTCTTG; for *WISP-1*: F:

TCATTAAGGCAGGGAAGAAG R: GTCTTAGACTTGTAGGGGATG; for BIRC3: F: ACAAGCAAGAGAACTGATTG R: GATCTGAAACATCTTCTGTGG and for Caspase 3 F: AAAGCACTGGAATGACATC R: CGCATCAATTCCACAATTTC. The amplification process included one cycle of 10 min at 95°C, 40 cycles for 15 s at 95°C, followed by 40 cycles for 1 min at 60°C. Thermal cycling and fluorescence detection were performed using an ABI 7500 Fast Prism (PE Applied Biosystems, Foster City, CA, USA).

Apoptosis gene expression array

HUVEC were cultured in 6-well plates until confluent and subjected to flow for 72 h using an orbital shaker. Following flow exposure, cells were washed twice with cold PBS and total DNA free mRNA was isolated using RNeasy Mini kits (Qiagen) and on-column DNase digestion as described above. mRNA integrity and concentration were determined spectrophotometrically. An RT2 Profiler^{tm} polymerase chain reaction (PCR) apoptosis array (PAHS-012ZA-Qiagen) was performed according to the manufacturer's instructions. Briefly, a total of 0.5 µg of RNA per sample was used with the RT2 First Strand kit (Qiagen) to obtain cDNA after incubation for 5 min with the gDNA elimination buffer. The PCR amplification process included one cycle of 10 min at 95°C, 40 cycles for 15 s at 95°C, followed by 40 cycles for 1 min at 60°C. Thermal cycling and fluorescence detection were performed using an ABI 7500 Fast Prism (PE Applied Biosystems, Foster City, CA, USA). The signals of the target cDNAs were normalized by comparison with the housekeeping genes HPRT1 supplied within the 96-well microtiter plate. The normalized amount of each target mRNA present in each condition was calculated using a comparative Ct method and using a web-based PCR array data analysis tool (https://www.qiagen.com/gb/shop/genes-and-pathways/data-analysis-center-overview-page/) with 1.5-fold difference set as baseline.

Statistical analysis

All data are presented as mean ± SEM. Statistical analysis was performed using GraphPad Prism software (v7.1). Statistical significance was assessed using paired two-tailed t-test (for

comparing two conditions) or by one-way analysis of variance (ANOVA) with repeated measures for multiple conditions. Each n is generated with a separate batch of ECs. For HUVEC these are pools of cells from different donors and for HAEC, in each batch EC had been isolated from a single donor. When using one-way ANOVA, tests for equal variance were run and if significantly different standard deviations were found (thus different variances) in the ANOVA with repeated measures a Gaussian distribution and no sphericity (not equal variability of the differences) was assumed and the Greenhouse-Geisser correction applied.

Results

β-catenin regulates eNOS activity in static HUVEC

To investigate whether β-catenin regulates eNOS activation in HUVEC, we assessed eNOS phosphorylation in cells following transfection with a pool of β-catenin siRNA oligonucleotides or an siRNA scrambled control pool. β-catenin depletion did not alter basal levels of eNOS phosphorylation (Figure 1A-B and S1A-B), however it did reduce agonist-induced eNOS phosphorylation on Ser1177 (Figure 1A and S1A). Interestingly, β-catenin depletion had no effect on agonist-induced eNOS phosphorylation on Ser633 (Figure 1B and S1B). Intracellular cGMP levels are a well-established indicator of bioactive NO levels; we observed that in HUVEC, the histamine-induced increase in cGMP production was reduced following depletion of β-catenin with siRNA (Figure 1C). The absence of β-catenin protein in HUVEC transfected with β-catenin siRNA was confirmed by western blotting (Figure S1C), furthermore, eNOS expression was not altered in β-catenin knockdown static cells (Figure S1D).

To confirm that β-catenin can promote eNOS phosphorylation on Ser1177 and thus increase NO and cGMP production, we treated HUVEC with LiCl that inhibits GSK3β-dependent phosphorylation of β-catenin and promotes its accumulation. We found that elevating β-

catenin levels with LiCl increased eNOS phosphorylation on Ser1177 but had no effect on Ser633 in static HUVEC (Figure 1D-F). Together these data demonstrate that β-catenin enhances agonist-dependent eNOS activation and subsequent cGMP production in HUVEC under static conditions.

β-catenin mediates the anti-apoptotic effects of NO-cGMP in static HUVEC

Since reduction of β-catenin may impair eNOS function and since NO is an important factor for EC survival[7], we assessed the potential protective effects of β-catenin, in relation to NO signalling, in static cultures following induction of apoptosis. In wild-type MPEC application of an NO donor (S-nitroso-N-acetylpenicillamine; SNAP) attenuated TNFα-induced apoptosis, indicated by a lower number of cleaved caspase-3 positive cells in the presence of SNAP, however in β-catenin$^{-/-}$ MPEC, the protective effects of SNAP on TNFα-induced apoptosis were abrogated (Figure 2A). We also examined TNFα-induced apoptosis in HUVEC and observed that siRNA depletion of β-catenin reduced the anti-apoptotic action of SNAP in this context (Figures 2B, 2E and S1E), demonstrating that β-catenin also mediates the pro-survival effects of NO in human EC under static conditions. Since β-catenin appears to regulate the level of activated eNOS and subsequent cGMP production in HUVEC, we examined activation of caspase-3 by H_2O_2 in HUVEC in the presence of sildenafil, a pharmacological sGC activator. Whilst cleaved caspase-3 levels induced by H_2O_2 are reduced by sildenafil treatment in scrambled control-treated cells, this was not the case in β-catenin depleted HUVEC (Figure 2C). Furthermore, ODQ, a pharmacological sGC inhibitor, abrogated the protective effects of SNAP in the presence of H_2O_2 (Figure 2D), indicating that NO exerts its anti-apoptotic effects through sGC activation and cGMP production. Together these data suggest that β-catenin mediates the pro-survival effects of NO and cGMP upon pharmacological (non-physiological) induction of apoptosis in static EC. eNOS expression and activation is known to increase in EC exposed to undisturbed flow[18] and enhanced endothelial NO synthesis promotes survival of EC under physiological levels of shear stress against TNFα and H_2O_2 [8,9]. For these reasons

we next sought to determine whether β-catenin mediates the pro-survival effects of NO under physiological flow conditions.

β-catenin associates with eNOS in HUVEC exposed to physiological flow

To confirm our previous observation made in static EC[15], and to test whether eNOS and β-catenin interact under physiological flow conditions, we carried out a proximity ligation assay (PLA) in HUVEC subjected to flow for 72h. We used an orbital shaking platform to generate reproducible spatially separated atheroprotective (undisturbed; uniaxial, high wall shear stress) and atheroprone (disturbed; multiaxial, low wall shear stress) flow patterns[17,18]. As previously described, HUVEC growing under atheroprotective, undisturbed flow (UF) were elongated and aligned meanwhile the cells in the atheroprone, disturbed flow (DF) central region showed a non-aligned mosaic-like morphology (Figure 3A and S2A). Furthermore, EC in the UF region expressed high levels of KLF2 and KLF4 and lower levels of MCP-1 and E-selectin compared to EC exposed to DF[20,21] (Figure S2B). Co-localization was observed in EC fixed and stained with anti-eNOS and anti-β-catenin antibodies (Figure S2A) and amplification products were detected by PLA indicating proximity (< 40nm) of both proteins in HUVEC exposed to both UF and DF (Figure 3A) but not in controls stained separately with either anti-eNOS or anti-β-catenin antibody. The average PLA signal per cell was lower in EC exposed to UF (Figure 3A) consistent with increased eNOS activity[15]. β-catenin and eNOS also co-localise *in vivo* in ECs of the inner and outer curvature of the aortic arch, regions of disturbed and undisturbed flow respectively, however co-localization was more prominent in the inner aortic arch (Figure 3B). In contrast with observations made in HUVEC subjected to acute low magnitude shear stress[22], no difference in the subcellular localization of β-catenin was observed in HUVEC exposed to chronic flow using an orbital shaker (Figure S2C).

β-catenin regulates eNOS phosphorylation in HUVEC exposed to physiological flow

Since activation of eNOS causes dissociation from β-catenin in static cells[15], the higher level of interaction observed in EC exposed to DF suggests lower activation of eNOS in these cells.

We thus measured eNOS phosphorylation on Ser1177, Ser633 and Ser114 and observed lower eNOS phosphorylation in EC exposed to DF compared to those exposed to UF (Figure 4A). To investigate whether β-catenin regulates eNOS activation in HUVEC exposed to flow, we assessed eNOS phosphorylation in HUVEC following transfection with β-catenin siRNA or a siRNA scrambled control and exposed to flow for 72h (Figure 4B). We observed that eNOS phosphorylation on Ser1177 decreased in EC exposed to UF when β-catenin was depleted but not in EC exposed to DF, consistent with our findings in static EC. eNOS expression was not altered by β-catenin knockdown, compared with scrambled control transfection, although eNOS expression was different in EC exposed to DF compared to UF (Figure S2D); but interestingly, phosphorylation on Ser114 was reduced in both UF and DF exposed HUVEC when β-catenin was depleted (Figure 4B). In contrast, treatment of HUVEC with LiCl increased Ser1177 phosphorylation in both regions (Figure 4C), confirming that β-catenin interacts with and can activate eNOS under physiological and atheroprone flow conditions.

Deletion of β-catenin increases apoptosis only in HUVEC exposed to disturbed flow

Atheroprotective, laminar flow activates eNOS and is the predominant source of NO in ECs. It has also been associated with EC survival[8,10]. In contrast, atherogenic shear stress profiles are associated with reduced expression of pro-survival genes and increased apoptosis, both *in vitro* and *in vivo*[23,24]. We measured apoptosis by cleaved caspase-3 staining of HUVEC subjected to flow using an orbital shaker and observed that the percentage of apoptosis was higher under DF compared to UF as expected (Figure S3A). Having established the involvement of β-catenin in NO-mediated anti-apoptotic activity in static cultures, we sought to determine the pro-survival actions of NO and β-catenin under physiological flow conditions. Inhibition of sGC activity with ODQ in HUVEC subjected to shear stress for 72h, increased apoptosis of HUVEC exposed to DF as assessed by cleaved caspase-3 immunostaining (Figure 5A). Furthermore, depletion of β-catenin in HUVEC promoted apoptosis exclusively in HUVEC exposed to DF (Figure 5B and S3B). In agreement with the higher level of apoptotic cells observed in DF exposed HUVEC, we also detected higher levels of cleaved caspase-3

in lysates from HUVEC subjected to DF for 72h (Figure S3C). Unexpectedly we found that the expression level of procaspase-3 (35 kDa) was lower in lysates from EC exposed to UF compared to DF (Figure 5C), though caspase-3 mRNA expression showed only a 20% increase in cells exposed to DF compared to UF (Figure S3D), suggesting that a post-translational mechanism may be regulating the protein expression and/or stability of caspase-3 in HUVEC exposed to UF.

Inhibition of β-catenin transcriptional activity increases apoptosis in HUVEC exposed to disturbed flow

Since β-catenin can regulate the expression of pro-survival genes and has also been shown to act downstream of eNOS/NO/cGMP, we investigated whether inhibiting its transcriptional activity also influenced cell survival under flow conditions. Inhibition of β-catenin-dependent transcriptional activation with the specific inhibitors of β-catenin/TCF-LEF interaction, iCRT5 or FH535[25,26], also exclusively increased apoptosis in HUVEC under DF in the same conditions (Figure 5D and S3E) and in HAEC exposed to DF (Figure S3F). The low level of apoptosis observed under UF was not altered by any method used to manipulate eNOS or β-catenin signalling (Figure 5A-E and S3E-G). Whilst treatment with histamine, which upregulates eNOS, reduced apoptosis in HUVEC exposed to DF (Figure 5E), inhibition of eNOS with 100mM L-NAME did not affect apoptosis in HUVEC exposed to either DF or UF (Figure S3G). These data indicate that signalling through sGC and β-catenin is essential to maintain cell survival in EC exposed to DF and that other additional mechanisms contribute to cell survival in UF-exposed HUVEC.

Inhibition of β-catenin-dependent transcription downregulates the expression of anti-apoptotic genes in HUVEC under flow

As the inhibition of cGMP signalling and β-catenin-dependent transcription increases apoptosis in HUVEC exposed to DF, we studied the expression of several anti-apoptotic genes that are potential targets of β-catenin: XIAP, WISP-1, Bcl-2 and survivin (BIRC5). Bcl-2 and

survivin exhibited differential expression between DF and UF regions in HUVEC (Figure 6A-B) as did eNOS (Figure 5C). Interestingly, survivin mRNA expression was reduced when cells were treated with iCRT5 or FH535, in HUVEC exposed to both UF and DF (Figure 6A and S4A). Bcl-2 and eNOS expression were also reduced in cells under UF in the presence of iCRT5. Treatment of HUVEC with ODQ also reduced the expression of eNOS (Figure 6D), suggesting the presence of a positive feedback mechanism in the eNOS-sGC-β-catenin pathway. WISP-1 showed very low expression in HUVEC and no differences were found in expression of XIAP between HUVEC exposed to UF and DF in the presence or absence of iCRT5 (not shown).

To identify novel putative genes regulating apoptosis and cell survival in EC exposed to flow, an apoptosis transcriptome array was performed with HUVEC exposed to UF or DF using an orbital shaker for 72h (Table S1). We classified the genes up- and downregulated in DF conditions according to the apoptotic pathways they regulate[27] and their function as shown in Table 1. We observed that the most significant change in EC exposed to DF was the downregulation of anti-apoptotic genes (Figure 6F and S5). These include members of the BCL and IAP (inhibitors of apoptosis) families including BIRC5 (survivin), NIAP1, BIRC-2 (cIAP-1), BIRC6, BCL2L2 and MCL-1. Although BIRC3 expression did not change from UF to DF, it was reduced in EC treated with iCRT5 (Figure S4B) and constitutes a novel target of β-catenin in EC. BIRC2 and BIRC3 are ubiquitin kinases which bind and promote caspase-3 inactivation and degradation[28]. We validated the expression of cIAP-1 by western blotting in HUVEC exposed to UF or DF (Figure S4C) and found its expression upregulated in UF-exposed HUVEC as expected, correlating with low levels of caspase-3 in UF-exposed EC. Treatment of cells with histamine, a pharmacological eNOS activator, that also promotes β-catenin nuclear translocation[15], reduced apoptosis in HUVEC exposed to DF (Figure 5E) and increased the level of survivin (Figure 6E) suggesting a central role for survivin in regulating cell survival in EC. Together these results support the central role of inhibitors of apoptosis,

and their positive regulation of expression by β-catenin, in mediating the pro-survival effects of the eNOS-cGMP pathway in EC exposed to flow.

Discussion

Phosphorylation of eNOS on Ser1177 is associated with increased eNOS activity and we show here in static EC that depletion of β-catenin reduced eNOS phosphorylation on Ser1177 in response to histamine and VEGF stimulation. We also demonstrated increased Ser1177 phosphorylation in EC exposed to UF and found that this was reduced following depletion of β-catenin. Stabilisation of β-catenin in HUVEC treated with LiCl increased Ser1177 phosphorylation in static and flow exposed EC. We conclude that β-catenin activates eNOS in human EC.

We previously reported that eNOS and β-catenin interact in static endothelial cells[15]. We show here that eNOS and β-catenin co-localise in regions of UF and DF in the mouse aorta *in vivo* with a higher degree of co-localization in the inner aortic arch region, supporting our finding that eNOS and β-catenin show a higher level of interaction in DF-exposed HUVEC *in vitro*. This may reflect higher eNOS activation under UF conditions and subsequent dissociation of the complex consistent with our finding that acute pharmacological activation of eNOS causes dissociation from β-catenin[15]. Since reduced levels of β-catenin associate with reduced eNOS phosphorylation in HUVEC, it may be that interaction of eNOS and β-catenin facilitates the access or recruitment of kinases that lead to phosphorylation of eNOS and subsequent dissociation of β-catenin from the complex. PKA and AKT are kinases that phosphorylate Ser1177 and activate eNOS in EC in response to different stimuli such as shear stress or VEGF treatment[29]. PKA and AKT also phosphorylate and stabilize β-catenin and enhance its transcriptional activity[30]. The identification of the putative kinases recruited by β-catenin to eNOS will be an important area of further study in order to understand the mechanism of action for the novel β-catenin dependent activation of eNOS described here.

We also demonstrate here that β-catenin and sGC signalling are essential mediators of the pro-survival effects of eNOS in static EC challenged with either TNFα or H_2O_2 to induce apoptosis. We previously reported that NO/GMP can stabilise β-catenin leading to transcriptional changes[15]. Furthermore, for the first time we present evidence showing that both NO-cGMP signalling and β-catenin transcriptional activity contribute to maintain cell survival in ECs under atheroprone flow conditions. HUVEC treated with the sGC inhibitor ODQ showed an increase in apoptosis in EC exposed to DF that was also observed in both HAEC and HUVEC treated with iCRT5, a specific inhibitor of β-catenin transcriptional activity. Our findings are supported by Saran *et al.*[31] who showed that the pro-apoptotic antagonist of Wnt signalling, sFRP4, causes endothelial dysfunction by suppressing NO-cGMP signalling.

Wnt/β-catenin promotes cell survival in static EC[32], but to our knowledge this is the first study to show that β-catenin regulates apoptosis in EC exposed to atheroprone disturbed flow. Several groups have studied the pro-survival and anti-apoptotic effects of undisturbed flow on EC[8,9] and identified GSH and NO as key regulators of cell survival in EC under atheroprotective flow conditions. Few studies have assessed the differential expression of the genes and signalling pathways regulating cell survival between disturbed and undisturbed flow[23,24,33]. Amini *et al.* demonstrated that JNK activity/expression was required to drive EC apoptosis at atheroprone sites in mice. Similarly, PERP, a p53 regulator was found to be upregulated in atheroprone areas of the porcine aorta, predisposing EC to apoptosis[33].

S-nitrosylation of β-catenin by iNOS can affect junctional permeability[34], a characteristic usually associated with EC exposed to DF. Recent findings suggest that β-catenin S-nitrosylation by eNOS impedes binding to the transcription factor TCF4[35]. This seems to be in contrast with our and others' findings suggesting that NO favours β-catenin separation from VE-cadherin and translocation to the cell nucleus[36]. In addition to NO, ROS production is necessary for S-nitrosylation in cells[37]. ROS increases in EC exposed to DF leading to low NO

bioavailability due to the reaction of ROS with NO to form peroxynitrite that promotes protein S-nitrosylation[38]. S-nitrosylation of β-catenin may explain the fact that we observe reduced levels of β-catenin dependent gene transcription in DF compared to UF exposed EC. Another interesting possibility that would need further investigation is that S-nitrosylation may allow β-catenin/TCF to discriminate certain promoters or would allow β-catenin interaction with a different member of the TCF family to activate cell survival vs proliferation programs (Axin2/ cyclinD1 vs anti-apoptotic genes).

β-catenin controls the transcriptional activation of several pro-survival and anti-apoptotic genes such as WISP-1, Bcl-2 and survivin in static cells[39,40]. Survivin has previously been shown to be downregulated in porcine aortic EC exposed to oscillatory flow[41] and Bcl-2 has been reported to be downregulated under low shear stress compared to high shear stress in HUVEC. Interestingly the expression of Bcl-2 in EC under high shear stress depends on eNOS activity[24]. Here we show that in HUVEC, survivin and Bcl-2 are upregulated in EC exposed to UF compared to DF, confirming the previous findings[24,40], and also that their expression is regulated by β-catenin under flow conditions. In addition, the expression of BIRC3, an inhibitor of apoptosis family member whose expression is flow independent, was also found to be positively regulated by β-catenin in HUVEC. Survivin has been identified as a key mediator of VEGF[40] and angiopoietin[42,43] induced survival; since both these stimuli activate eNOS activity their anti-apoptotic actions may be mediated via an NO-driven increase in β-catenin activation and consequent increase in the transcription of pro-survival/anti-apoptotic genes. We also observed that survivin expression increased with histamine treatment in HUVEC. The correlation between survivin expression in EC under flow with NO and β-catenin levels further supports our finding that β-catenin is a novel mediator of the pro-survival effects of NO, possibly via regulation of survivin and Bcl-2 expression. Although our experiments have identified clear changes in survivin and Bcl-2 transcript expression, in future work such changes in expression will need confirmation also at the protein level.

Despite the decreased expression of Bcl-2 and survivin in EC exposed to UF following inhibition of β-catenin, we saw no accompanying increase in apoptosis. This finding suggested that other redundant mechanisms exist in cells exposed to UF that protect the cells from pro-apoptotic stimuli resulting in a powerful pro-survival phenotype. Interestingly we found that the expression of pro-caspase-3 was extremely low in HUVEC exposed to UF when compared to DF conditions. Since caspase-3 is considered the main executioner caspase in EC, this may be a parallel regulatory mechanism limiting apoptosis in EC exposed to UF. Caspases are regulated post-translationally by IAPs (inhibitors of apoptosis), a family of E3 ubiquitin ligases. In particular caspase-3 activity is regulated by BIRC2 (cIAP1) and BIRC3 (cIAP2), that ubiquitinate caspases and promote inactivation and/or subsequent degradation by the proteasome[44]. In HUVEC, cIAP1 which is upregulated by high shear stress was also shown to cause a decrease in caspase-3 activity, although caspase expression was not assessed[45]. Here we describe for the first time that protein levels of caspase-3 are decreased in EC exposed to atheroprotective UF. In our mRNA apoptosis array, BIRC2 (cIAP1) was upregulated under UF compared to DF and protein expression was confirmed by western blotting, suggesting that high levels of cIAP1 in EC exposed to UF may contribute to the degradation and loss of caspase-3 in these cells.

Our data suggests a bidirectional regulation of the eNOS-β-catenin interaction. Upon eNOS activation, β-catenin translocates to the nucleus to activate gene transcription but β-catenin also promotes eNOS activation suggesting that activation of one of the pathways will activate the other one providing a cross talk between the Wnt/β-catenin and NO. In future work, it would be instructive to also investigate the role of caspases -8 and -9, which are upstream of caspase-3, as well as the functional relevance of caspase activation, for example by the use of pharmacological inhibitors, in the apoptosis pathways investigated here. It will also be important to dissect in further detail the effects on eNOS phosphorylation observed in our study, by assaying individual kinases. Nevertheless, our data provide strong evidence of an

interaction between two well-established pro-survival pathways and we propose that the eNOS-cGMP-β-catenin axis is essential to maintain cell survival in EC under disturbed flow.

Acknowledgements

We thank the Nikon Imaging Center@King's College London (John Harris, Dan Matthews and Isma Ali) for help with microscopy, the Genomics Centre at King's College London for help with qPCR, and Drs Sarah Chapple and Giovanni Mann in the School of Cardiovascular Medicine & Sciences at King's College London for providing the mice used in this study. This work was supported by a grant from the British Heart Foundation to AF and CW (PG/15/116/31947).

Conflicts of interest

None declared.

References

1. Lee, Y. & Gustafsson, A.B. Role of apoptosis in cardiovascular disease. *Apoptosis* **14,** 536-548 (2009).
2. Tricot, O. et al. Relation between endothelial cell apoptosis and blood flow direction in human atherosclerotic plaques. *Circulation* **101,** 2450-2453 (2000).
3. Bombeli, T., Schwartz, B.R. & Harlan, J.M. Endothelial cells undergoing apoptosis become proadhesive for nonactivated platelets. *Blood* **93,** 3831-3838 (1999).
4. Cancel, L.M. & Tarbell, J.M. The role of apoptosis in LDL transport through cultured endothelial cell monolayers. *Atherosclerosis* **208,** 335-341 (2010).
5. Lyons, D. Impairment and restoration of nitric oxide-dependent vasodilation in cardiovascular disease. *Int. J. Cardiol.* **62 Suppl 2,** S101-S109 (1997).
6. Cannon, R.O. 3rd. Role of nitric oxide in cardiovascular disease: focus on the endothelium. *Clin. Chem.* **44,** 1809-1819 (1998).
7. Dimmeler, S. & Zeiher, A.M. Nitric oxide-an endothelial cell survival factor. *Cell Death Differ.* **6,** 964-968 (1999).
8. Dimmeler, S., Haendeler, J., Nehls, M. & Zeiher, A.M. Suppression of apoptosis by nitric oxide via inhibition of interleukin-1beta-converting enzyme (ICE)-like and cysteine protease protein (CPP)-32-like proteases. *J. Exp. Med.* **185,** 601-607 (1997).
9. Hermann, C., Zeiher, A.M. & Dimmeler, S. Shear stress inhibits H2O2-induced apoptosis of human endothelial cells by modulation of the glutathione redox cycle and nitric oxide synthase. *Arterioscler. Thromb. Vasc. Biol.* **17,** 3588-3592 (1997).
10. Dimmeler, S., Rippmann, V., Weiland, U., Haendeler, J. & Zeiher, A.M. Angiotensin II induces apoptosis of human endothelial cells. Protective effect of nitric oxide. *Circ. Res.* **81,** 970-976 (1997).

11. Hoffmann, J. et al. Aging enhances the sensitivity of endothelial cells toward apoptotic stimuli: important role of nitric oxide. *Circ. Res.* **89,** 709-715 (2001).

12. Rossig, L. et al. Nitric oxide inhibits caspase-3 by S-nitrosation in vivo. *J. Biol. Chem.* **274,** 6823-6826 (1999).

13. Rossig, L. et al. Nitric oxide down-regulates MKP-3 mRNA levels: involvement in endothelial cell protection from apoptosis. *J. Biol. Chem.* **275,** 25502-25507 (2000).

14. Hebestreit, H. et al. Disruption of fas receptor signaling by nitric oxide in eosinophils. *J. Exp. Med.* **187,** 415-425 (1998).

15. Warboys, C.M. et al. Bidirectional cross-regulation between the endothelial nitric oxide synthase and beta-catenin signalling pathways. *Cardiovasc. Res.* **104,** 116-126 (2014).

16. MacDonald, B.T., Tamai, K. & He, X. Wnt/beta-catenin signaling: components, mechanisms, and diseases. *Dev. Cell* **17,** 9-26 (2009).

17. Ghim, M. et al. Visualization of three pathways for macromolecule transport across cultured endothelium and their modification by flow. *Am. J. Physiol. Heart Circ. Physiol.* **313,** H959-H973 (2017).

18. Warboys, C.M. et al. Disturbed flow promotes endothelial senescence via a p53-dependent pathway. *Arterioscler. Thromb. Vasc. Biol.* **34,** 985-995 (2014).

19. Gavrieli, Y., Sherman, Y. & Ben-Sasson, S.A. Identification of programmed cell death in situ via specific labeling of nuclear DNA fragmentation. *J. Cell Biol.* **119,** 493-501 (1992).

20. Sangwung, P. et al. KLF2 and KLF4 control endothelial identity and vascular integrity. *JCI Insight* **2,** e91700 (2017).

21. Dardik, A. et al. Differential effects of orbital and laminar shear stress on endothelial cells. *J. Vasc. Surg.* **41,** 869-880 (2005).

22. Sheng, X. et al. Effects of FSS on the expression and localization of the core proteins in two Wnt signaling pathways, and their association with ciliogenesis. *Int. J. Mol. Med.* **42,** 1809-1818 (2018).

23. Amini, N. et al. Requirement of JNK1 for endothelial cell injury in atherogenesis. *Atherosclerosis* **235,** 613-618 (2014).

24. Bartling, B. et al. Shear stress-dependent expression of apoptosis-regulating genes in endothelial cells. *Biochem. Biophys. Res. Commun.* **278,** 740-746 (2000).

25. Gonsalves, F.C. et al. An RNAi-based chemical genetic screen identifies three small-molecule inhibitors of the Wnt/wingless signaling pathway. *Proc. Natl Acad. Sci. USA* **108,** 5954-5963 (2011).

26. Handeli, S. & Simon, J.A. A small-molecule inhibitor of Tcf/beta-catenin signaling down-regulates PPARgamma and PPARdelta activities. *Mol. Cancer Ther.* **7,** 521-529 (2008).

27. Elmore, S. Apoptosis: a review of programmed cell death. *Toxicol. Pathol.* **35,** 495-516 (2007).

28. Vaux, D.L. & Silke, J. IAPs, RINGs and ubiquitylation. *Nat. Rev. Mol. Cell Biol.* **6,** 287-297 (2005).

29. Heiss, E.H. & Dirsch, V.M. Regulation of eNOS Enzyme Activity by Posttranslational Modification. *Curr. Pharm. Des.* **20,** 3503-3513 (2014).

30. Hino, S., Tanji, C., Nakayama, K.I. & Kikuchi, A. Phosphorylation of beta-catenin by cyclic AMP-dependent protein kinase stabilizes beta-catenin through inhibition of its ubiquitination. *Mol. Cell Biol.* **25,** 9063-9072 (2005).

31. Saran, U. et al. sFRP4 signalling of apoptosis and angiostasis uses nitric oxide-cGMP-permeability axis of endothelium. *Nitric Oxide* **66,** 30-42 (2017).

32. Masckauchan, T.N., Shawber, C.J., Funahashi, Y., Li, C.M. & Kitajewski, J. Wnt/beta-catenin signaling induces proliferation, survival and interleukin-8 in human endothelial cells. *Angiogenesis* **8,** 43-51 (2005).

33. Serbanovic-Canic, J. et al. Zebrafish Model for Functional Screening of Flow-Responsive Genes. *Arterioscler. Thromb. Vasc. Biol.* **37,** 130-143 (2017).

34. Thibeault, S. et al. S-nitrosylation of beta-catenin by eNOS-derived NO promotes VEGF-induced endothelial cell permeability. *Mol. Cell* **39,** 468-476 (2010).

35. Zhang, Y., Chidiac, R., Delisle, C. & Gratton, J.P. Endothelial NO Synthase-Dependent S-Nitrosylation of beta-Catenin Prevents Its Association with TCF4 and Inhibits Proliferation of Endothelial Cells Stimulated by Wnt3a. *Mol. Cell Biol.* **37,** e00089-17 (2017).

36. Mei, J.M., Borchert, G.L., Donald, S.P. & Phang, J.M. Matrix metalloproteinase(s) mediate(s) NO-induced dissociation of beta-catenin from membrane bound E-cadherin and formation of nuclear beta-catenin/LEF-1 complex. *Carcinogenesis* **23,** 2119-2122 (2002).

37. Yang, Y. & Loscalzo, J. S-nitrosoprotein formation and localization in endothelial cells. *Proc. Natl Acad. Sci. USA* **102,** 117-122 (2005).

38. Hsieh, H.J., Liu, C.A., Huang, B., Tseng, A.H. & Wang, D.L. Shear-induced endothelial mechanotransduction: the interplay between reactive oxygen species (ROS) and nitric oxide (NO) and the pathophysiological implications. *J. Biomed. Sci.* **21,** 3 (2014).

39. Pennica, D. et al. WISP genes are members of the connective tissue growth factor family that are up-regulated in wnt-1-transformed cells and aberrantly expressed in human colon tumors. *Proc. Natl Acad. Sci. USA* **95,** 14717-14722 (1998).

40. Kaga, S., Zhan, L., Altaf, E. & Maulik, N. Glycogen synthase kinase-3beta/beta-catenin promotes angiogenic and anti-apoptotic signaling through the induction of VEGF, Bcl-2 and survivin expression in rat ischemic preconditioned myocardium. *J. Mol. Cell. Cardiol.* **40,** 138-147 (2006).

41. Himburg, H.A., Dowd, S.E. & Friedman, M.H. Frequency-dependent response of the vascular endothelium to pulsatile shear stress. *Am. J. Physiol. Heart Circ. Physiol.* **293,** H645-653 (2007).

42. Papapetropoulos, A. et al. Angiopoietin-1 inhibits endothelial cell apoptosis via the Akt/survivin pathway. *J. Biol. Chem.* **275,** 9102-9105 (2000).

43. Ahmed, A. et al. Angiopoietin-2 confers Atheroprotection in apoE-/- mice by inhibiting LDL oxidation via nitric oxide. *Circ. Res.* **104,** 1333-1336 (2009).

44. Choi, Y.E. et al. The E3 ubiquitin ligase cIAP1 binds and ubiquitinates caspase-3 and -7 via unique mechanisms at distinct steps in their processing. *J. Biol. Chem.* **284,** 12772-12782 (2009).

45. Jin, X., Mitsumata, M., Yamane, T. & Yoshida, Y. Induction of human inhibitor of apoptosis protein-2 by shear stress in endothelial cells. *FEBS Lett.* **529,** 286-292 (2002).

Tables

Table 1: Apoptosis genes regulated by UF and DF in HUVEC

Extrinsic Pathway (Death Receptor)	UF	DF	*p-value*	Fold regulation
Receptors and positive regulators				
TNFRSF25 (DR3)	2.0240	0.5587	0.0005	-3.6224
TNFRSF7 (CD27)	0.0702	0.0214	0.0098	-3.2806
TNFRSF6 (FAS)	1.0081	0.4273	0.0001	-2.4041
TNFSF6 (FASLG)	0.0194	0.0095	0.0033	-2.0387
TNFSF5 (CD40LG)	0.0466	0.0237	0.0136	-1.9686
TNFRSF1A (TNFR1)	6.8953	3.7187	0.0265	-1.8542
TNFRSF10B (DR5)	7.3743	4.4220	0.0210	-1.6939
TRAF2	0.6532	0.4123	0.0290	-1.5841
Negative regulators				
CFLAR (cFLIP/Casper)	11.0632	5.2331	0.0005	-2.1141
IL10	0.0046	0.0022	0.0449	-2.0572
Intrinsic Pathway (Mitochondrial/DNA Damage)	**NT UF**	**NT DF**	***p-value***	**Fold regulation**
Positive regulators				
BCL2L11	0.3164	0.6653	0.0008	2.1026
PYCARD	0.9250	1.9230	0.0067	2.0788
CYCS	0.2805	0.1124	0.0003	-2.4964
APAF1	2.1224	0.9547	0.0032	-2.2230
BIK	0.0158	0.0075	0.0019	-2.1070
TP53BP2	2.2696	1.1816	0.0059	-1.9209
AIFM1	1.2792	0.6753	0.0265	-1.8542
BAK1	0.6385	0.4079	0.0240	-1.5654
Negative regulators				
BRAF	0.2838	0.1096	0.0001	-2.5910
BCL2L2	3.6138	1.5032	0.0006	-2.4041
BAG1	0.1032	0.0459	0.0281	-2.2514
MCL1	16.5490	10.5281	0.0263	-1.5719
Executioners	**NT UF**	**NT DF**	***p-value***	**Fold regulation**
NOD1	2.3301	1.0904	0.0001	-2.1370
Caspase 10	2.8597	1.5029	0.0008	-1.9028
Caspase 9	0.9849	0.5731	0.0044	-1.7186
Caspase 8	0.4631	0.2622	0.0067	-1.7663
CIDEB	1.5123	0.8723	0.0228	-1.7336
ABL1	2.3718	1.5154	0.0207	-1.5651
Inhibitors and Negative regulators				
BIRC1 (NAIP)	2.4156	0.6697	0.0015	-3.6072
BIRC6	4.1225	1.5979	0.0001	-2.5799
BIRC2	5.5505	2.7168	0.0007	-2.0430
BIRC5 (Survivin)	0.1991	0.1175	0.0210	-1.6939
NOL3	0.8344	0.5255	0.0061	-1.5877

Gene names are indicated and common synonyms are shown in brackets. UF and DF represent fold change (2^-ΔΔCt) in mRNA expression compared to the housekeeping gene (HPRT1)in non-treated HUVEC exposed to UF or DF for 72h, n=3. Fold-regulation is the negative inverse of the fold-change. Fold regulation values greater than one indicates up-regulation and fold-regulation values less than one indicate down-regulation. In red are indicated genes that can behave like anti or pro-apoptotic depending on alternative splicing.

Figure Legends

Figure 1. β-catenin depletion inhibits agonist induced eNOS phosphorylation in static HUVEC. (A-C) HUVEC were transfected with siRNA targeting β-catenin (100 nM) or scrambled control siRNA (Scr) and cultured for 72h before treatment for 5 min with vehicle or histamine (100 mmol/L). Cell lysates were analysed by western blot using total eNOS, b-catenin, phospho-Ser1177 **(A)** or phospho-Ser633 **(B)** antibodies. **(C)** cGMP levels were quantified by ELISA and results expressed relative to protein content per sample (shown relative to scrambled control; n=4). **(D-F)** HUVEC were cultured for 72h before treatment for the indicated times with vehicle or LiCl (20mM). Cell lysates were analysed by western blot using total eNOS, phospho-Ser1177 **(D)** or phospho-Ser633 **(E)** and b-catenin **(F)** antibodies. **(A,B,D,E)** Results expressed as the densitometric ratio of phospho-eNOS/GAPDH to total eNOS/GAPDH and shown relative to untreated control (n=5); analysis by one-way ANOVA with repeated measures, ns: non significant, *p≤0.05, **p≤0.01, ***p≤0.001.

Figure 2. β-catenin mediates the anti-apoptotic effects of NO in static HUVEC. **(A)** Wild-type and β-catenin$^{-/-}$ MPECs were treated with SNAP (10 μM) or vehicle. **(B)** HUVEC were transfected with siRNA targeting β-catenin (100 nM) or scrambled control and cultured for 72h before treatment with TNFα (10 ng/ml) for 18h in the presence or absence of SNAP (10 μM). **(A-B)** EC were fixed and incubated with anti-cleaved caspase-3 antibody and DAPI. Representative images are shown. The percentage of cleaved caspase-3 positive cells was calculated in 5 randomly selected fields of view (n=4). **(C)** HUVEC were transfected with siRNA targeting β-catenin (100 nM) or scrambled control and cultured for 72h before treatment with H_2O_2 (200 μM) for 6h in the presence or absence of sildenafil (50 nM; n=4). The bands shown by way of example are from the same experiment. **(D)** HUVEC were treated with H_2O_2 (200 μM) for 6h in the presence of SNAP (10 μM), ODQ (10μM) or both in combination (n=3). **(C-D)** Cleaved (17kDa and 19kDa) and full length (35kDa) caspase-3 were detected in western blots of cell lysates and normalised to β-actin. Densitometry values are shown expressed

relative to vehicle control. **(E)** HUVEC were transfected with siRNA targeting β-catenin (100 nM) or scrambled control and cultured for 72h before treatment with H_2O_2 (200 μM) for 6h in the presence or absence of SNAP (10 μM, following which cells were fixed and DNA fragmentation assessed using a Click-IT TUNEL Imaging Kit (n=5), All analyses by one-way ANOVA with repeated measures, ns non-significant, *p≤0.05, **p≤0.01, ***p≤0.001. Scale bars show 100 mm.

Figure 3: β-catenin interacts with eNOS under flow. (A) HUVEC were exposed to orbital flow for 72h, fixed and subject to PLA using antibodies targeting eNOS and b-catenin. In control samples PLA was carried out in the absence of b-catenin (I) or eNOS antibody (II). VE-cadherin and DAPI were used to stain cell junctions and nuclei, respectively. Representative images are shown and the average PLA signal quantified in HUVEC under disturbed flow (DF) or undisturbed flow (UF; n=4); analysis by paired Student's t–test, **p≤0.01. **(B)** EC from protected (outer curvature) or atherosusceptible (inner curvature) regions of the mouse aorta were stained with eNOS (red) and β-catenin (green) antibodies and imaged en face by confocal microscopy. Merged representative images with DAPI (blue) are shown (n=3). Scale bars show 50 mm.

Figure 4: β-catenin regulates eNOS under flow. (A) Cell lysates were obtained from HUVEC exposed to UF or DF for 72h (n=4). **(B)** EC transfected with non-targeting scrambled or β-catenin targeting siRNA (100 nM) were exposed to orbital flow for 72h (n=5). **(C)** Cell lysates obtained from HUVEC exposed to UF or DF for 72h and treated with vehicle or LiCl (20mM) for the last 4h (n=3). **(A-C**) Cell lysates were analysed by western blot with the indicated antibodies. Results are expressed as the densitometric ratio of phospho-eNOS/eNOS to total eNOS/calnexin and shown relative to levels in UF in vehicle or scr treated

conditions; analysis by paired Student's t–test **(A)** or analysis by one-way ANOVA with repeated measures **(B-C)**, *p≤0.05, **p≤0.01, ***p≤0.001.

Figure 5: Inhibition of sGC and β-catenin transcriptional activity increases apoptosis in HUVEC exposed to disturbed flow. (A-E) HUVEC were exposed to orbital flow for 72h and treated with DMSO, ODQ (10mM) **(A)**, iCRT5 (50 mM) **(D)** or Histamine (100 mmol/L) **(E)** for the last 24h of flow exposure or transfected with b-catenin or Scr siRNA (100nM) **(B)**. **(B)** ECs were fixed and incubated with a cleaved caspase-3 antibody (green), anti-b-catenin (red) and nuclei stained with DAPI. Representative images are shown. **(A,B,D,E)** The percentage of cleaved caspase-3 positive cells was quantified in regions of undisturbed (UF) or disturbed flow (DF) (n=3-7). **(C)** HUVEC were exposed to orbital flow or static conditions for 72h. Full length (35 kDa) caspase-3 was detected in western blots of cell lysates. Results are expressed as the densitometric ratio of caspase-3 to calnexin. Representative western blots are shown (right panel) (n=9); analysis by paired Student's t–test **(C)** or analysis by one-way ANOVA with repeated measures **(A-B,D-E)**, *p≤0.05, **p≤0.01, ***p≤0.001. Scale bars show 50 mm.

Figure 6. Inhibition of β-catenin downregulates the expression of survivin and Bcl-2 in HUVEC exposed to flow. (A-F) HUVEC were exposed to orbital flow for 72h and treated with DMSO or iCRT5 (50 μM) **(A-C)**, ODQ (10 mM) **(D)** or histamine (100 mM) **(E)** for the last 24h of flow or left untreated **(F)**. Transcript levels of survivin **(A,E)**, Bcl-2 **(B)** and eNOS **(C-D)** were assessed in HUVEC under disturbed flow (DF) or undisturbed flow (UF) by qRT–PCR using GAPDH as a housekeeping gene. Values are shown relative to expression in vehicle treated HUVEC under UF; analysis by ANOVA with repeated measures (n=3-4); n.s., not significant, *p≤0.05, **p≤0.01, ***p≤0.001. **(F)** mRNA samples from HUVEC exposed to DF or UF were analysed using an mRNA expression array targeting 84 apoptotic related genes. HPRT1 was used as housekeeping gene (n=3). The Volcano plot shows expression fold change of mean

across replicates in each condition from DF to UF on x axis (log2) and p-value (-log10) on y axis. Significantly differentially expressed genes (p-value < 0.05) are highlighted in red (up-regulated FC>1.5) or green (down-regulated; FC<-1.5). Relevant genes are indicated.

Figure 1

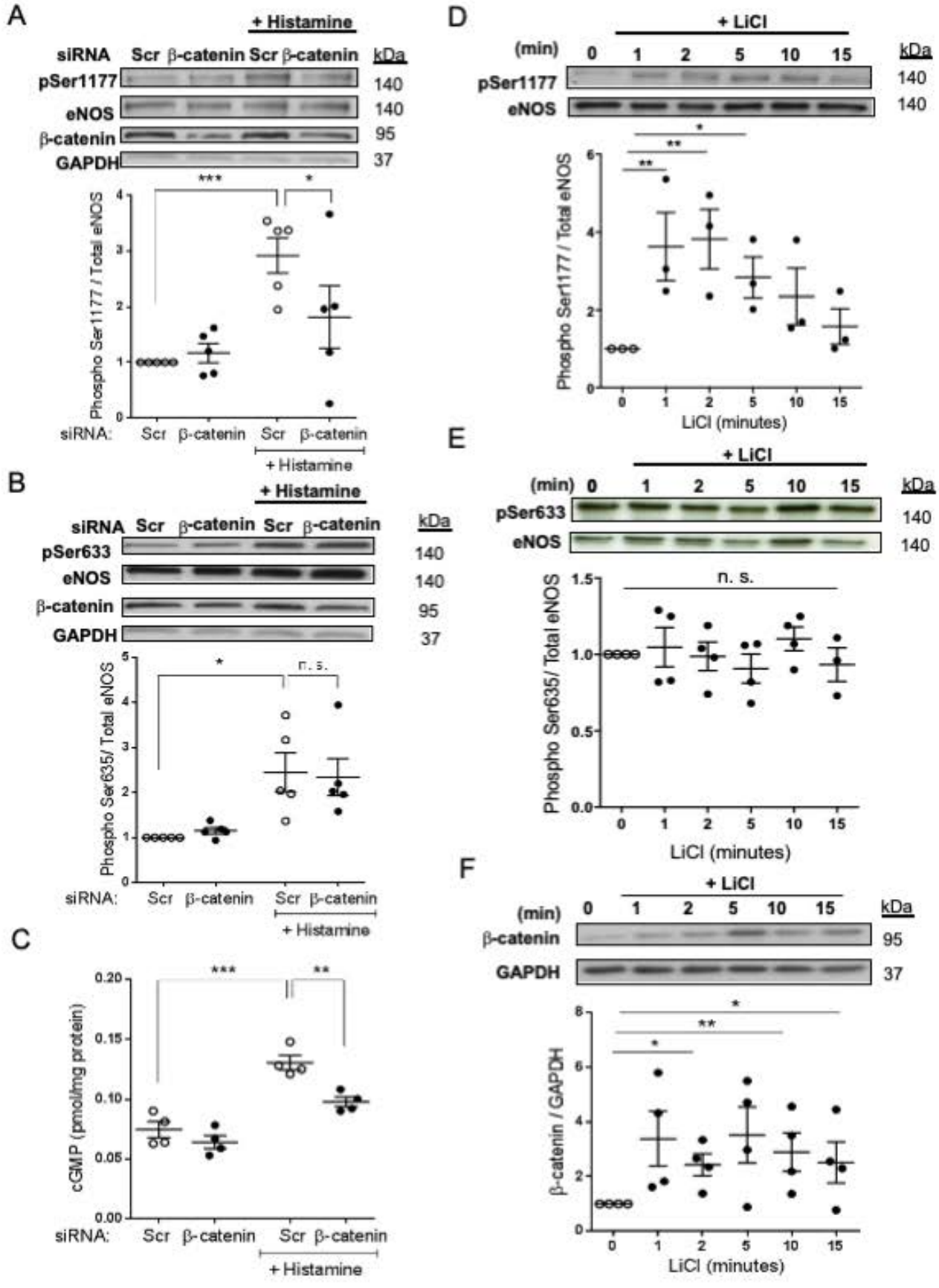
A
+ Histamine
siRNA Scr β-catenin Scr β-catenin kDa
pSer1177 140
eNOS 140
β-catenin 95
GAPDH 37
Phospho Ser1177 / Total eNOS
siRNA: Scr β-catenin Scr β-catenin
+ Histamine
B
+ Histamine
siRNA Scr β-catenin Scr β-catenin kDa
pSer633 140
eNOS 140
β-catenin 95
GAPDH 37
Phospho Ser635/ Total eNOS
n. s.
siRNA: Scr β-catenin Scr β-catenin
+ Histamine
C
cGMP (pmol/mg protein)
siRNA: Scr β-catenin Scr β-catenin
+ Histamine
D
+ LiCl
(min) 0 1 2 5 10 15 kDa
pSer1177 140
eNOS 140
Phospho Ser1177 / Total eNOS
LiCl (minutes)
E
+ LiCl
(min) 0 1 2 5 10 15 kDa
pSer633 140
eNOS 140
n. s.
Phospho Ser635/ Total eNOS
LiCl (minutes)
F
+ LiCl
(min) 0 1 2 5 10 15 kDa
β-catenin 95
GAPDH 37
β-catenin / GAPDH
LiCl (minutes)

Figure 2

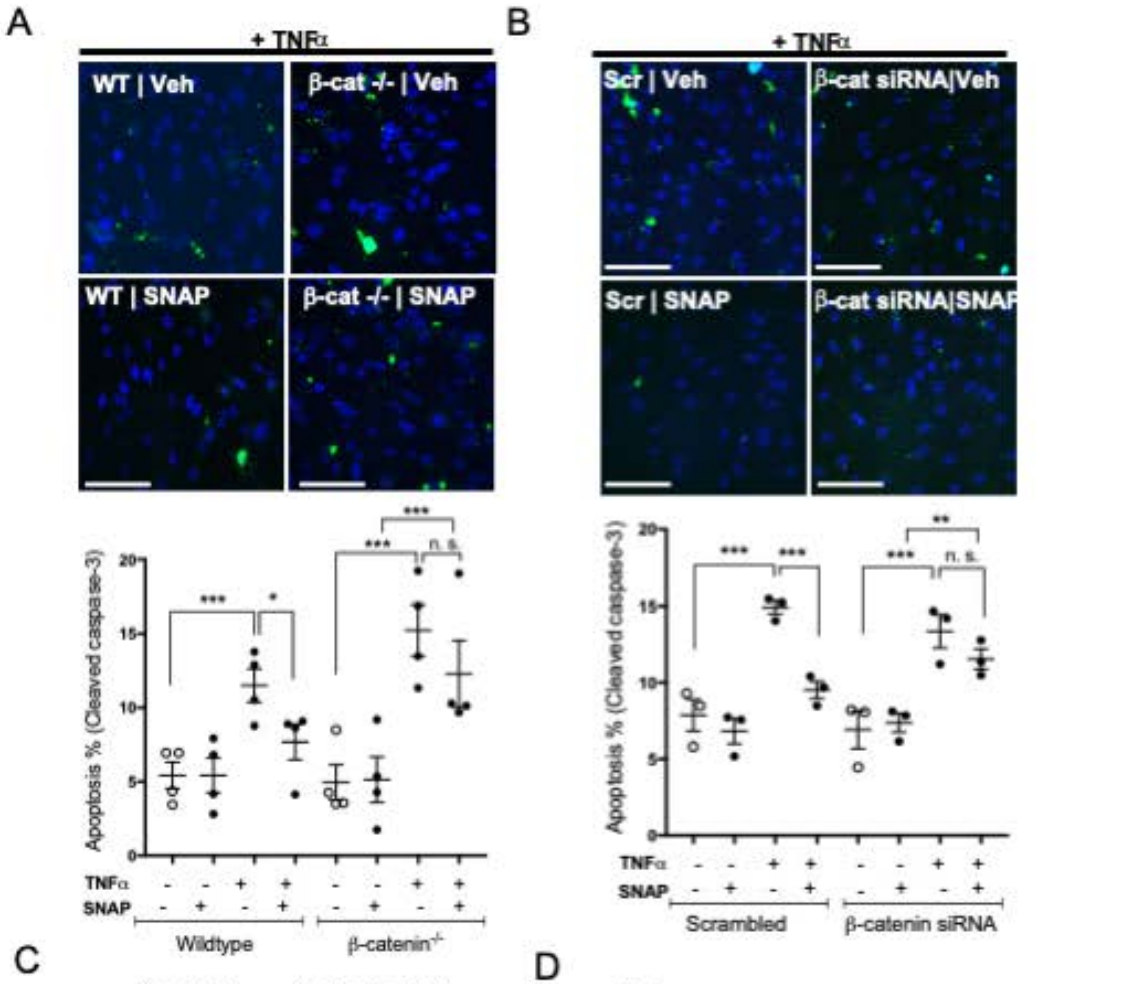
A
+ TNFα
WT | Veh
β-cat -/- | Veh
WT | SNAP
β-cat -/- | SNAP
Apoptosis % (Cleaved caspase-3)
TNFα
SNAP
Wildtype
β-catenin-/-
B
+ TNFα
Scr | Veh
β-cat siRNA|Veh
Scr | SNAP
β-cat siRNA|SNAP
Apoptosis % (Cleaved caspase-3)
TNFα
SNAP
Scrambled
β-catenin siRNA

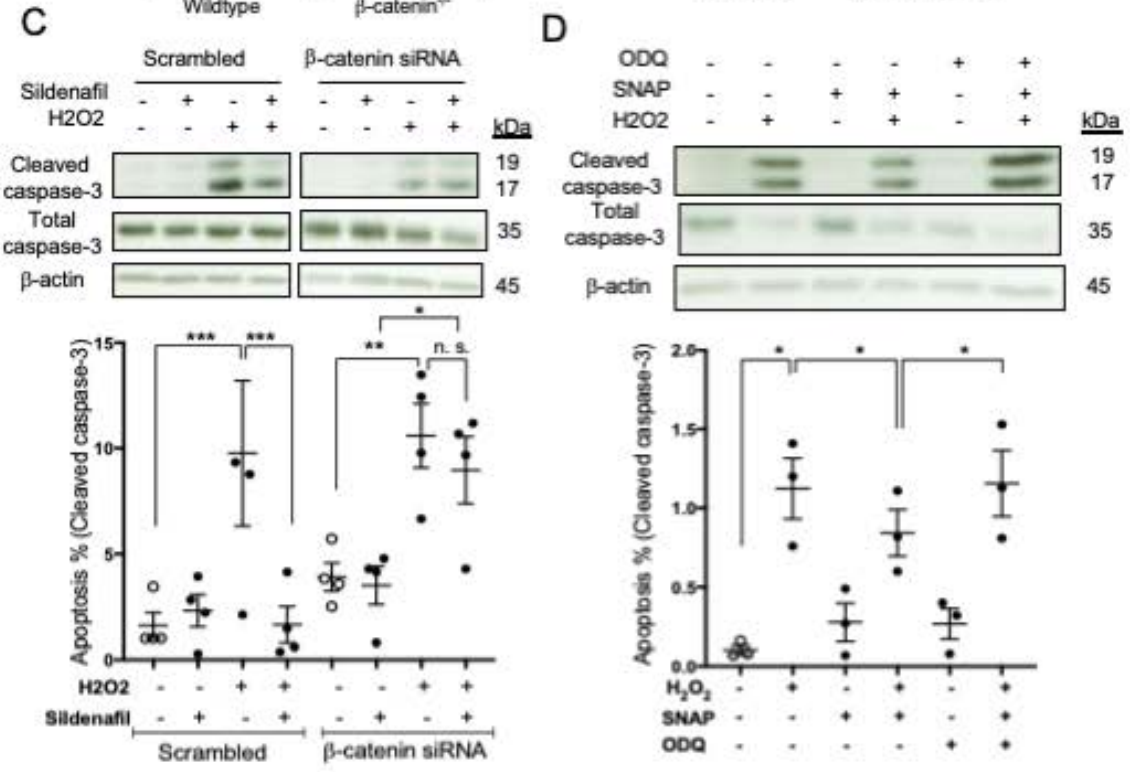
C
Scrambled
β-catenin siRNA
Sildenafil
H2O2
kDa
Cleaved caspase-3
Total caspase-3
β-actin
19
17
35
45
Apoptosis % (Cleaved caspase-3)
H2O2
Sildenafil
Scrambled
β-catenin siRNA
D
ODQ
SNAP
H2O2
kDa
Cleaved caspase-3
Total caspase-3
β-actin
19
17
35
45
Apoptosis % (Cleaved caspase-3)
H2O2
SNAP
ODQ

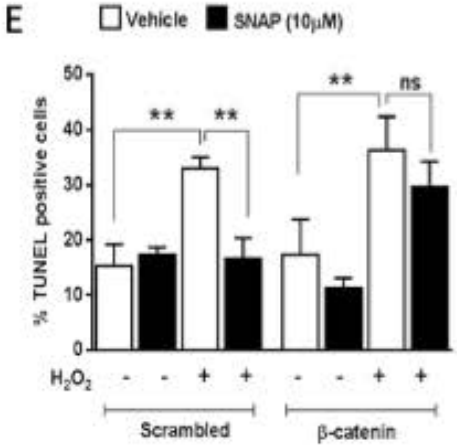
E
Vehicle
SNAP (10μM)
% TUNEL positive cells
H2O2
Scrambled
β-catenin

Figure 3

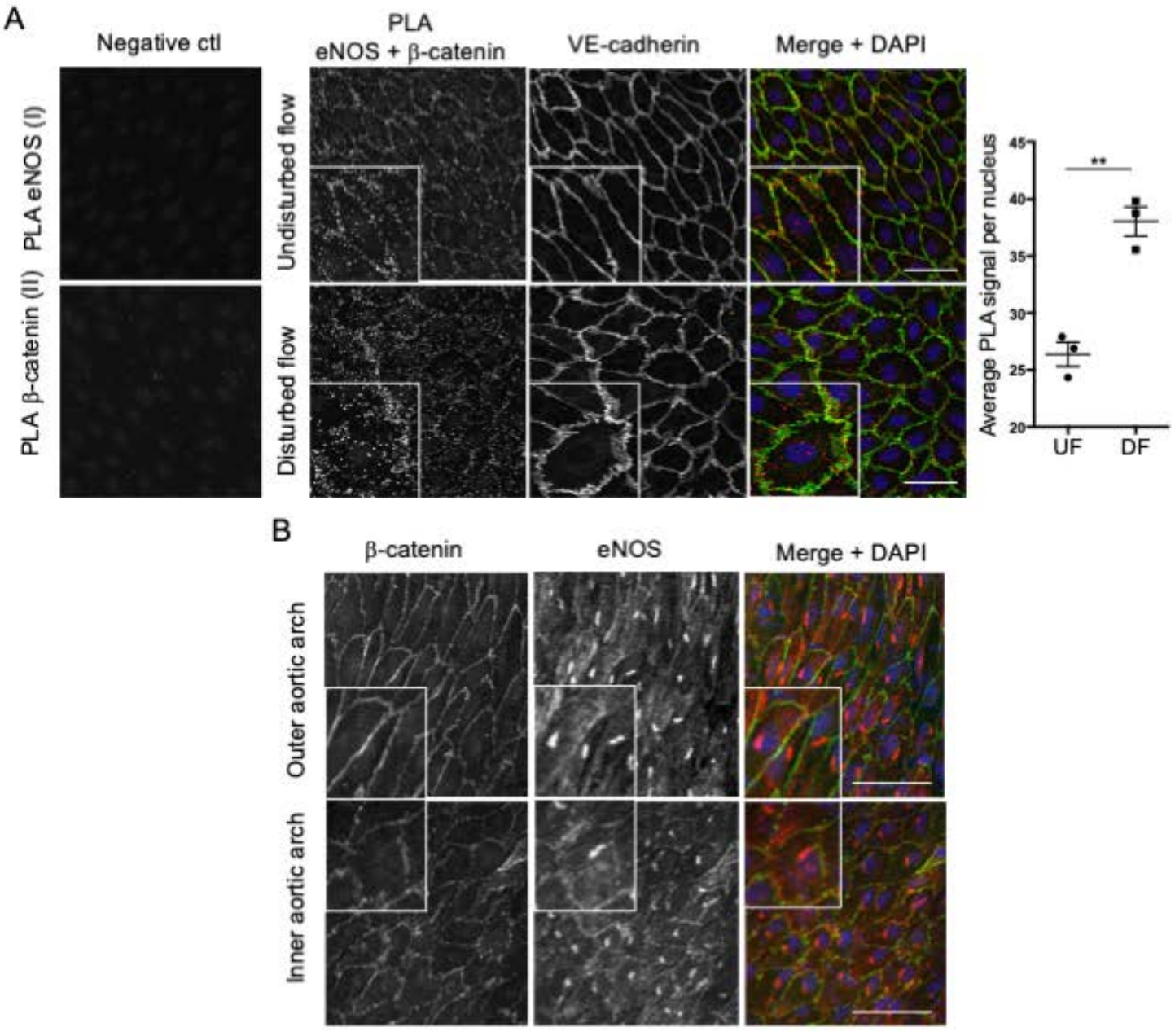
A
Negative ctl
PLA
eNOS + β-catenin
VE-cadherin
Merge + DAPI
PLA eNOS (I)
PLA β-catenin (II)
Undisturbed flow
Disturbed flow
Average PLA signal per nucleus
45
40
35
30
25
20
**
UF
DF
B
β-catenin
eNOS
Merge + DAPI
Outer aortic arch
Inner aortic arch

Figure 4

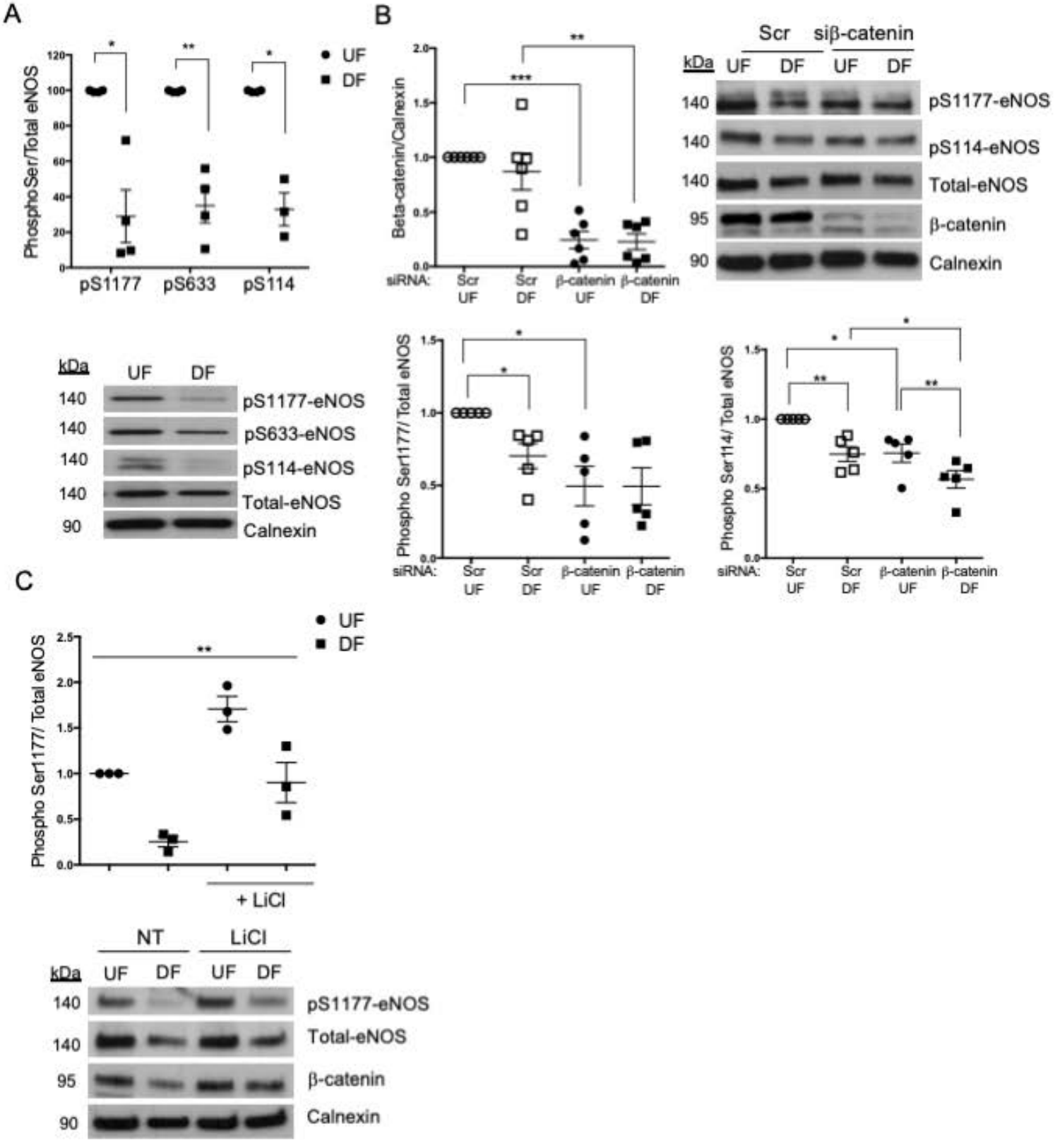
A
Phospho Ser/Total eNOS
UF
DF
pS1177
pS633
pS114
kDa
UF
DF
140
pS1177-eNOS
140
pS633-eNOS
140
pS114-eNOS
140
Total-eNOS
90
Calnexin
B
Beta-catenin/Calnexin
siRNA:
Scr UF
Scr DF
β-catenin UF
β-catenin DF
Scr
siβ-catenin
pS1177-eNOS
pS114-eNOS
Total-eNOS
β-catenin
Calnexin
Phospho Ser1177/ Total eNOS
Phospho Ser114/ Total eNOS
C
Phospho Ser1177/ Total eNOS
+ LiCl
NT
LiCl
pS1177-eNOS
Total-eNOS
β-catenin
Calnexin

Figure 5

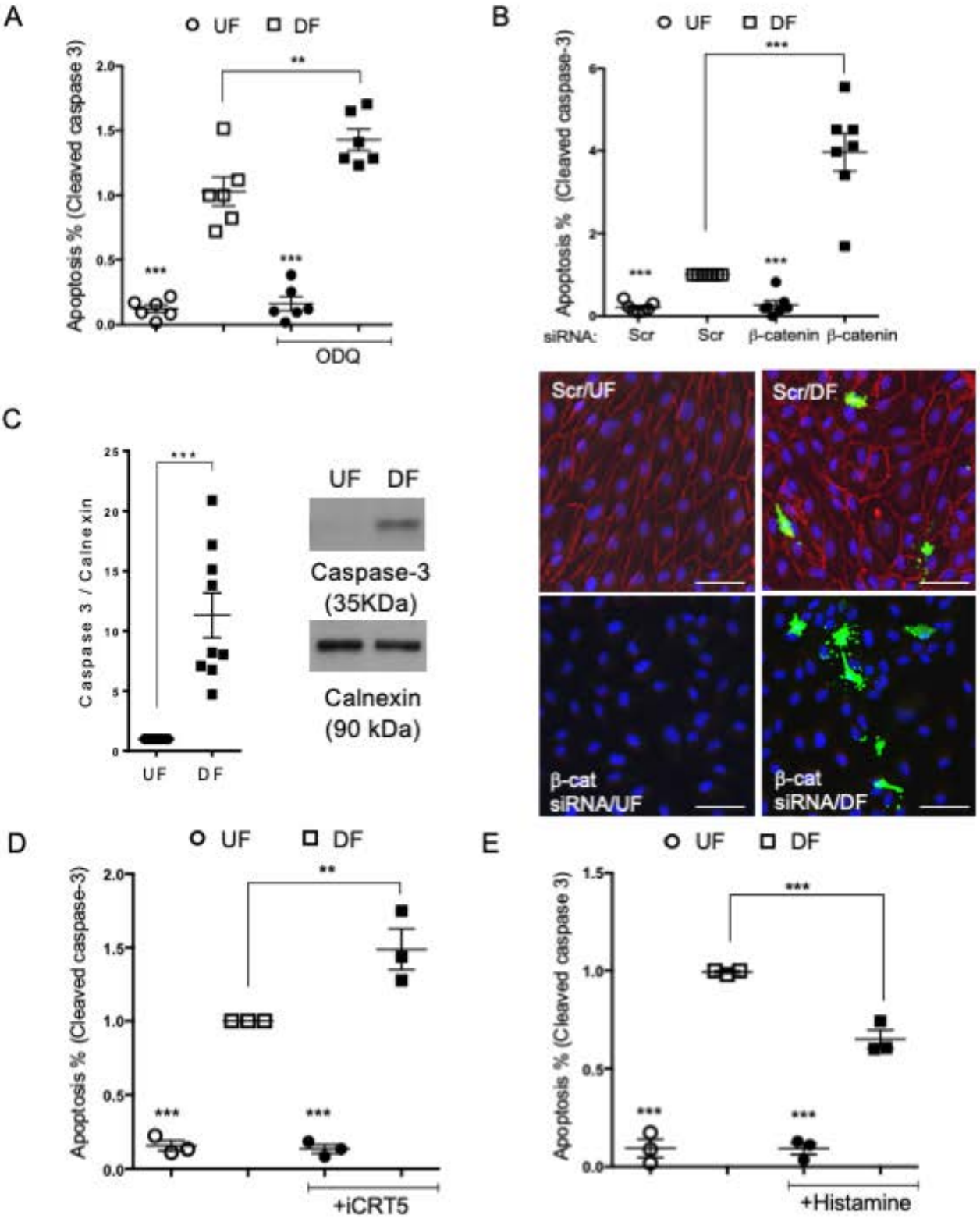
A
UF
DF
Apoptosis % (Cleaved caspase 3)
ODQ
B
Apoptosis % (Cleaved caspase-3)
siRNA:
Scr
Scr
β-catenin
β-catenin
Scr/UF
Scr/DF
β-cat siRNA/UF
β-cat siRNA/DF
C
Caspase 3 / Calnexin
Caspase-3 (35KDa)
Calnexin (90 kDa)
D
+iCRT5
E
+Histamine

Figure 6

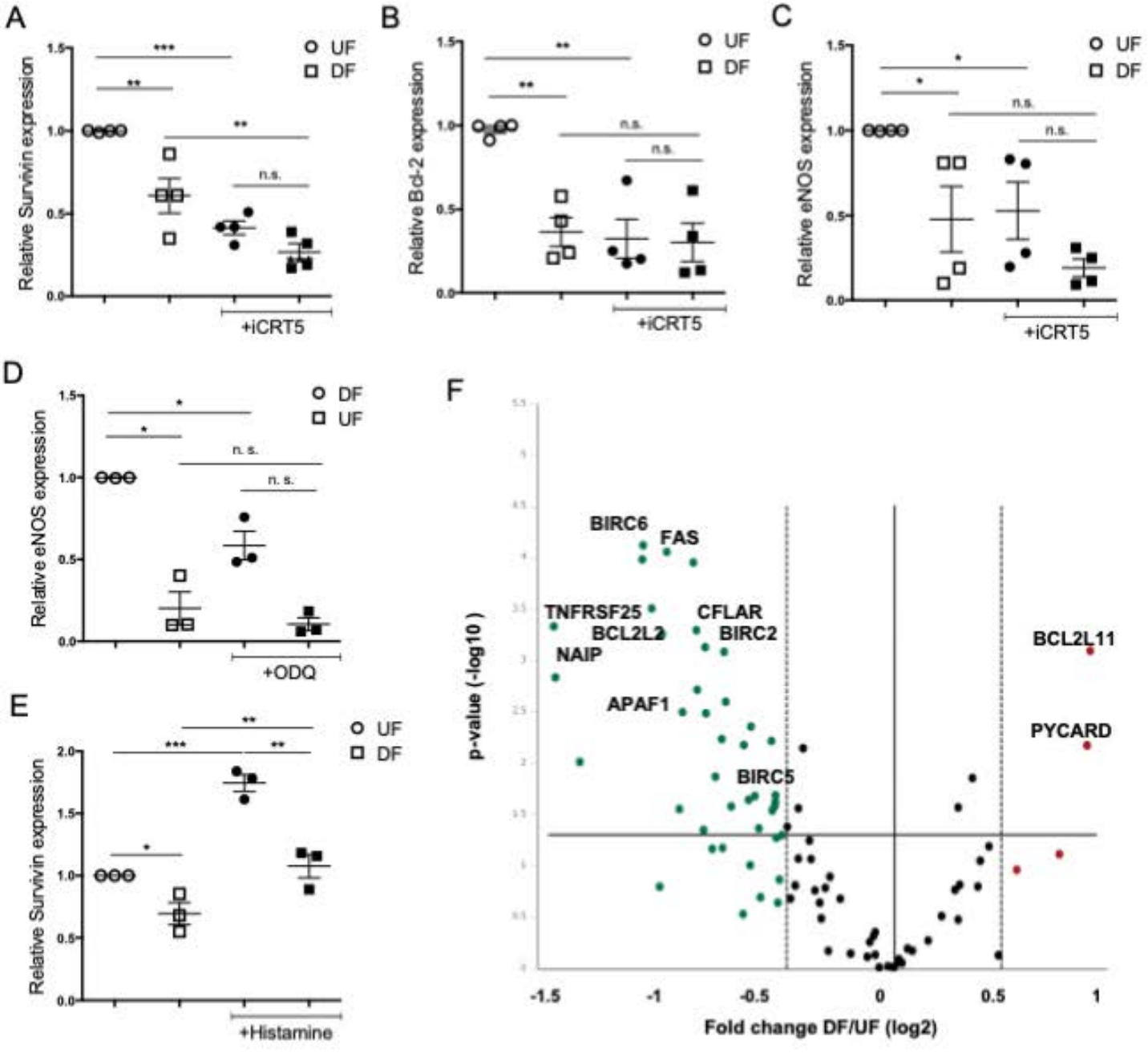
A
Relative Survivin expression
UF
DF
+iCRT5
B
Relative Bcl-2 expression
UF
DF
+iCRT5
C
Relative eNOS expression
UF
DF
+iCRT5
D
Relative eNOS expression
DF
UF
+ODQ
E
Relative Survivin expression
UF
DF
+Histamine
F
p-value (-log10)
Fold change DF/UF (log2)
BIRC6
FAS
TNFRSF25
CFLAR
BCL2L2
BIRC2
NAIP
APAF1
BIRC5
BCL2L11
PYCARD

β-catenin promotes endothelial survival by regulating eNOS activity and flow-dependent anti-apoptotic gene expression

Virginia Tajadura[1], Marie Haugsten Hansen[1], Joy Smith[1], Hannah Charles[1], Matthew Rickman[2], Keith Farrell-Dillon[1], Vasco Claro[1], Christina Warboys[2,3*] and Albert Ferro[1*]

[1]School of Cardiovascular Medicine & Sciences, British Heart Foundation Centre of Research Excellence, King's College London, London SE1 9NH, UK
[2]Department of Bioengineering, Imperial College London, London, SW7 2BP, UK
[3] Department of Comparative Biomedical Sciences, Royal Veterinary College, London, NW1 0TU, UK

**Joint corresponding author*

Supplementary Figures and Table

Supplementary Figure S1: β-catenin depletion inhibits agonist induced eNOS phosphorylation in static HUVEC. (A-B) HUVEC were transfected with siRNA targeting β-catenin or scrambled control (Scr) and cultured for 72h before treatment for 5 min with vehicle or VEGF (20 nmol/L). Cell lysates were analysed by western blot using anti-β-catenin, total eNOS, phospho-Ser1177 (A) or phospho-Ser633 (B) antibodies. Results expressed as the densitometric ratio of phospho-eNOS/GAPDH to total eNOS/GAPDH (A-B) and shown relative to untreated scrambled control (n=5); analysis by one-way ANOVA with repeated measures, n s: non significant, *p≤0.05, **p≤0.01, ***p≤0.001. (C-E) Cell lysates from non treated HUVEC transfected with siRNA targeting β-catenin or scrambled control (Scr) were analysed by western blot using anti-β-catenin (C,E) total eNOS (D) and GAPDH antibodies and bands quantified by densitometry (n=22); analysis by paired student t-test (C-E) or ANOVA with repeated measures (A-B); n.s., not significant, *p≤0.05, **p≤0.01, ***p≤0.001.

Supplementary Figure S2: eNOS and β-catenin co-localize in HUVEC. (A) HUVEC were exposed to orbital flow for 72h, fixed and stained with eNOS (green), β-catenin (red) and DAPI (blue) antibodies. Representative images are shown of HUVEC either in the periphery of the well (Undisturbed flow) or in the centre of the well (Disturbed flow). Scale bar represents 50μm. (B) HUVEC were exposed to orbital flow for 72h and mRNA samples prepared from EC either in the periphery of the well (UF) or in the centre of the well (DF). Transcript levels of KLF2 and E-Selectin (ESEL) were assessed by quantitative RT–PCR using GAPDH as a housekeeping gene (n=3). (C) Lysates from HUVEC exposed to orbital flow for 72h were obtained and separation into a soluble cytoplasm+membrane and nuclear fractions was performed. Lysates were analysed by western blotting using β-catenin, lamin B1 and PECAM1 antibodies. Densitometry values for the cytoplasmic (β-catenin/PECAM-1) and the nuclear (β-catenin/ lamin B1) fractions are shown relative to UF. Representative western blots are shown in right panel (n=4). (D) EC transfected with non-targeting scrambled or β-catenin targeting siRNA (100 nM) were exposed to orbital flow for 72h. Lysates obtained from UF and DF exposed

cells were analysed by western blotting, (n=5). Analysis by paired Student's t–test (B-C) or analysis by ANOVA with repeated measures (D), n s: non significant, *p≤0.05, **p≤0.01.

Supplementary Figure S3: β-catenin regulates apoptosis in EC exposed to flow. (A) HUVEC were exposed to orbital flow for 72h, fixed and stained with cleaved caspase 3 (green), active β-catenin (red) and DAPI (blue) antibodies. Representative images are shown of HUVEC either in the periphery of the well (UF) or in the centre of the well (DF). Scale bar shows 25μm. (B) EC transfected with non-targeting scrambled or β-catenin targeting siRNA (100 nM) were exposed to orbital flow and cell lysates analysed by western blot (n=6). (C) Lysates from HUVEC exposed to UF or DF for 72h were immunoblotted with caspase 3 and calnexin antibodies. Densitometry values are shown relative to UF. Representative western blots with calnexin and cleaved caspase 3 (17kDa) are shown in right panel (n=3). (D) HUVEC were exposed to orbital flow for 72h and mRNA samples prepared from EC either in the periphery of the well (UF) or in the centre of the well (DF). Transcript levels of caspase 3 were assessed by quantitative RT–PCR using GAPDH as a housekeeping gene (n=3). (E) HUVEC were exposed to orbital flow for 72h and treated with FH535 (50 μM) or DMSO for the last 24h. EC were fixed and incubated with an antibody that detects the cleaved form of caspase-3 (Asp175) and nuclei stained with DAPI. The percentage of cleaved caspase-3 positive cells was calculated in the periphery of the well (UF) and in the centre of the cell (DF). Values are shown relative to vehicle treated DF (n=3). (F) HAEC were exposed to orbital flow for 72h and treated with iCRT5 (50 μM) or DMSO for the last 24h. The relative rate of apoptosis was quantified as in D (n=5). (G) HUVEC were exposed to orbital flow for 72h and treated with L-NAME (100 μM) or left untreated for the last 24h and the relative rate of apoptosis was quantified as in D (n=4); analysis by paired Student's t–test (B-D) or ANOVA with repeated measures (E-G); n s: non-significant, *p≤0.05, **p≤0.01, ***p≤0.001.

Supplementary Figure S4: Inhibitors of apoptosis are downregulated in DF exposed HUVEC. (A) HUVEC were exposed to orbital flow for 72h and treated with FH535 (25 μM) or DMSO for the last 24h. Transcript levels of survivin were assessed by quantitative RT–PCR using GAPDH as a housekeeping gene. Values are shown relative to DMSO (n=3). (B) HUVEC were exposed to orbital flow for 72h and treated with iCRT5 (50 μM) or DMSO for the last 24h. Transcript levels of BIRC3 were assessed as in B (n=3). (C) HUVEC were exposed to orbital flow for 72h and protein levels of BIRC2 were assessed in HUVEC under disturbed flow (DF) or undisturbed flow (UF) by western blot. Values are shown relative to expression in EC under UF. Right panel shows blot representative of n=3; analysis by paired Student's t–test (A,C) or one-way ANOVA with repeated measures (B); n s: non significant, *p≤0.05, ***p≤0.001).

Supplementary Figure S5: Anti-apoptotic genes are down-regulated in EC exposed to disturbed flow. HUVEC were exposed to orbital flow for 72h and mRNA samples prepared from EC either in the periphery of the well (UF) or in the centre of the well (DF). An mRNA expression array targeting 84 apoptotic related genes was performed. HPRT1 was used as housekeeping gene (n=3). Significantly differentially expressed genes with a p-value < 0.05 and with a FC>1.5 or FC<-1.5 were selected as hits. (A) 39% of the genes tested (33 out of 84) showed at least a 1.5-fold change in expression between DF and UF conditions. Of those, 31 were genes downregulated in EC exposed to DF compared to UF and only 2 genes were found to be upregulated. Of the 84 genes tested, 19 encoded death receptors or ligands, 19 encoded anti-apoptotic or pro-survival proteins, 27 encoded pro-apoptotic factors, 15 encoded effector caspases and other downstream executor proteins [27] and 4 encoded proteins that can be pro- or anti-apoptotic (Supplementary Table S1). Both of the genes that were upregulated in DF conditions, encoded pro-apoptotic proteins. Of the genes found to be downregulated, 35.4% (11 out of 31) encoded anti-apoptotic or pro-survival proteins, 22.5% (7 out of 31) pro-apoptotic proteins, 22.5% (7 out of 31) death receptors and 18% (6 out of 31)

caspases and other executor proteins. The anti-apoptotic genes downregulated in EC exposed to DF constitute 57.8% of the anti-apoptotic genes included in the array (11 out of 19) meanwhile the other genes represented 26.9%, 36.8 % and 33% of the pro-apoptotic, receptors and ligands or effector genes tested respectively. (B) Pie chart showing the number of hits in each category.

Supplementary Table S1: Summary of apoptosis-related gene expression in HUVEC exposed to UF and DF.

Supplementary Figure S1

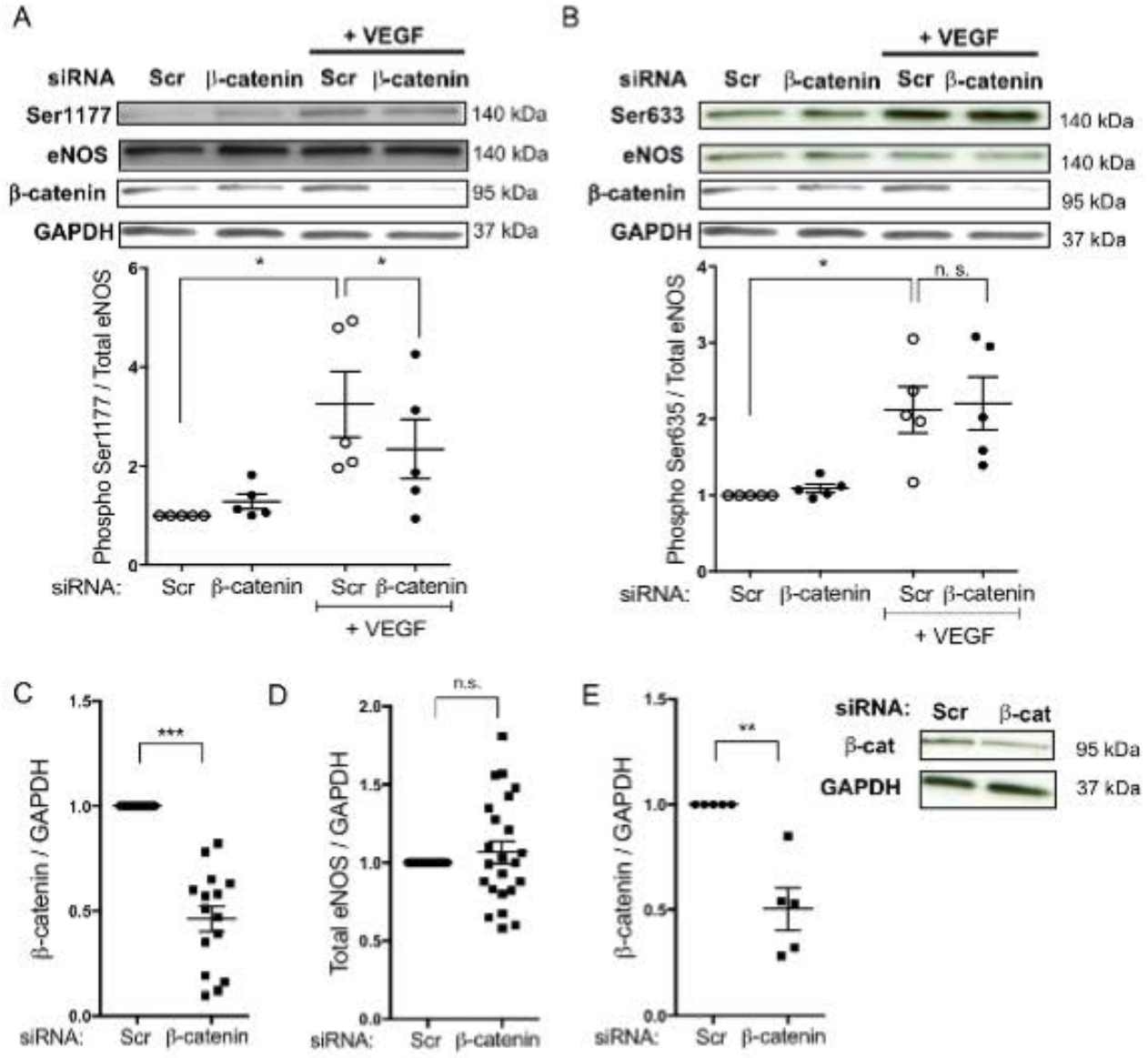

Supplementary Figure S2

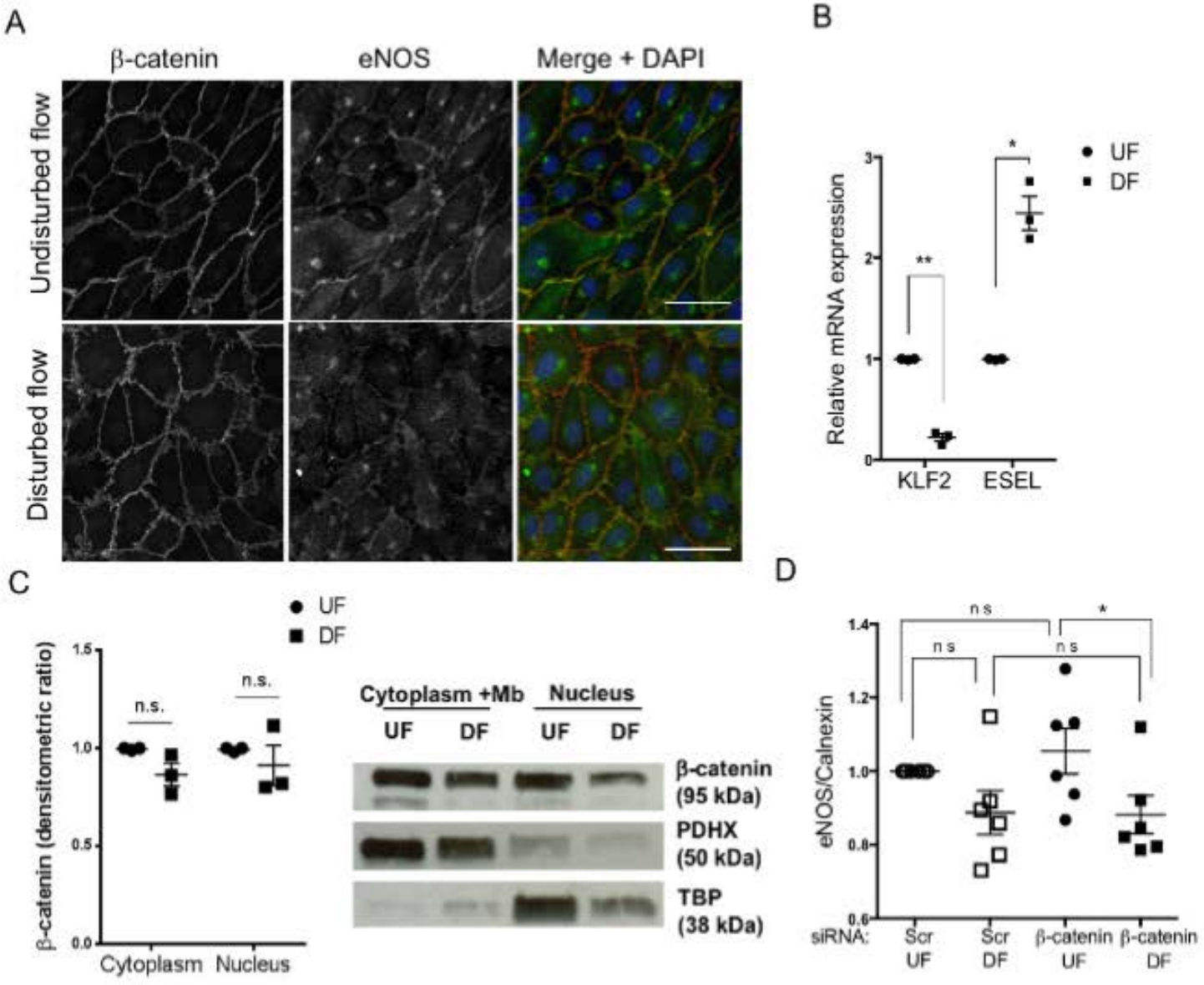

Supplementary Figure S3

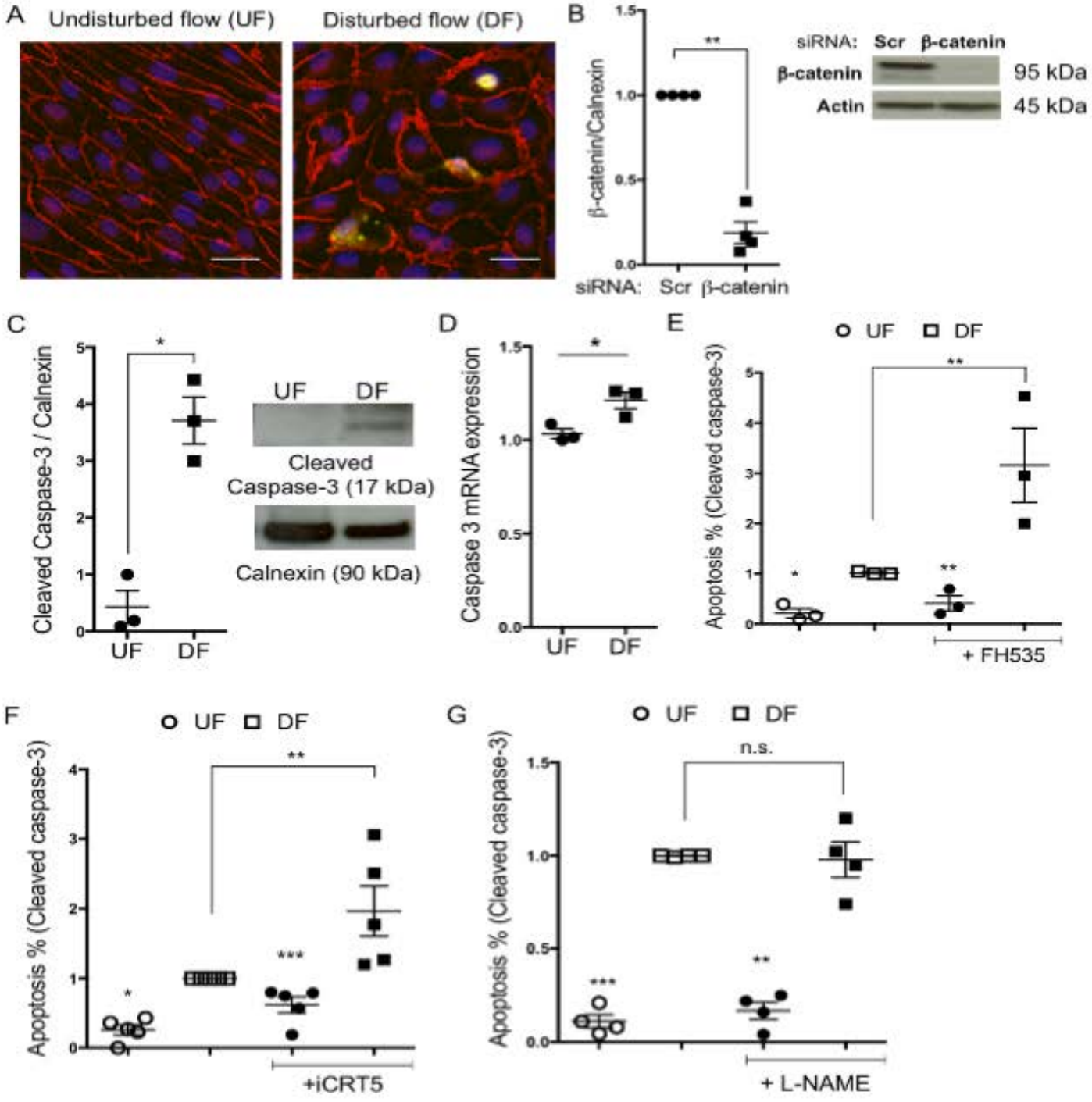

Supplementary Figure S4

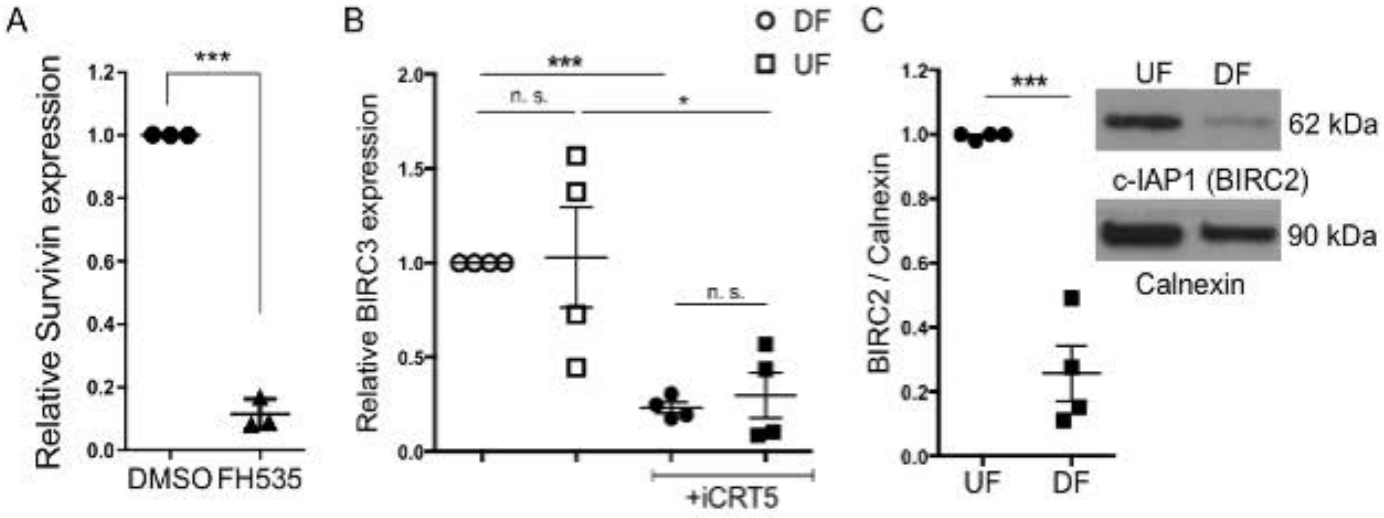

Supplementary Figure S5

A

	Death receptors	Anti apoptotic	Pro apoptotic	Effectors	Bivalent regulators	TOTAL
Number of genes tested	**19**	**19**	**27**	**15**	**4**	**84**
% of total genes tested	22.6	22.6	32.1	17.8	4.7	**99.8**
Number of genes down-reg in DF	**7**	**11**	**8**	**5**		**31**
% of genes down-reg	22.5	35.4	25.8	16.1		**99.8**
% of genes in category	36.8	57.8	26.9	33.3		**N/A**
% of total genes tested	8.3	13	9.5	5.9		**36.7**
Number of genes up-reg in DF			**2**			**2**
% of genes up-reg			100			**100**
% of genes in category			7.4			**N/A**
% of total genes tested			2.3			**2.3**

B

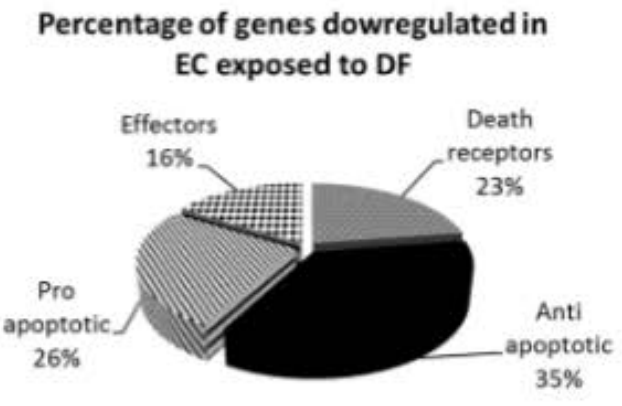

				Fold Regulation	*p-value*
Position	**Refseq**	**Symbol**	**Apoptotic pathway/category**	**DF vs UF**	***DF vs UF***
A01	NM_005157	ABL1	Pro-apoptotic	-1.5651	*0.02068*
A02	NM_004208	AIFM1	Pro-apoptotic	-1.8943	*0.002535*
A03	NM_005163	AKT1	Anti-apoptotic/pro-survival	1.1985	*0.308315*
A04	NM_001160	APAF1	Pro-apoptotic	-2.223	*0.003211*
A05	NM_004322	BAD	Pro-apoptotic	1.3863	*0.089515*
A06	NM_004323	BAG1	Anti-apoptotic/pro-survival	-2.2514	*0.028103*
A07	NM_004281	BAG3	Anti-apoptotic/pro-survival	-1.4116	*0.007195*
A08	NM_001188	BAK1	Pro-apoptotic	-1.5654	*0.023977*
A09	NM_004324	BAX	Pro-apoptotic	-1.0736	*0.736664*
A10	NM_003921	BCL10	Pro-apoptotic	1.0144	*0.868758*
A11	NM_000633	BCL2	Anti-apoptotic/pro-survival	-1.3674	*0.086221*
A12	NM_004049	BCL2A1	Anti-apoptotic/pro-survival	-2.4236	*0.159624*
B01	NM_138578	BCL2L1	Anti-apoptotic/pro-survival	1.001	*0.972438*
B02	NM_020396	BCL2L10	Pro-apoptotic	-1.1049	*0.768924*
B03	NM_006538	BCL2L11	Pro-apoptotic	2.1026	*0.000809*
B04	NM_004050	BCL2L2	Anti-apoptotic/pro-survival	-2.4041	*0.000559*
B05	NM_016561	BFAR	Bifunctional (Pro/Anti-apoptotic)	-1.2742	*0.127776*
B06	NM_001196	BID	Pro-apoptotic	1.0543	*0.641333*
B07	NM_001197	BIK	Pro-apoptotic	-2.107	*0.001943*
B08	NM_001166	BIRC2	Anti-apoptotic/pro-survival	-2.043	*0.000747*
B09	NM_001165	BIRC3	Anti-apoptotic/pro-survival	-1.0248	*0.952439*
B10	NM_001168	BIRC5	Anti-apoptotic/pro-survival	-1.6939	*0.020966*
B11	NM_016252	BIRC6	Anti-apoptotic/pro-survival	-2.5799	*0.000076*

B12	NM_004330	BNIP2	Bifunctional (Pro/Anti-apoptotic)	-1.3498	*0.173635*
C01	NM_004052	BNIP3	Bifunctional (Pro/Anti-apoptotic)	1.2745	*0.027125*
C02	NM_004331	BNIP3L	Bifunctional (Pro/Anti-apoptotic)	1.2849	*0.153039*
C03	NM_004333	BRAF	Pro-apoptotic	-2.591	*0.000104*
C04	NM_033292	CASP1	Executor and effector proteins	-1.226	*0.209515*
C05	NM_001230	CASP10	Executor and effector proteins	-1.9028	*0.000829*
C06	NM_012114	CASP14	Executor and effector proteins	-1.5276	*0.050478*
C07	NM_032982	CASP2	Executor and effector proteins	-1.4381	*0.085554*
C08	NM_004346	CASP3	Executor and effector proteins	-1.5627	*0.053641*
C09	NM_001225	CASP4	Executor and effector proteins	-1.0731	*0.442365*
C10	NM_004347	CASP5	Executor and effector proteins	-1.7717	*0.295184*
C11	NM_032992	CASP6	Executor and effector proteins	-1.095	*0.552437*
C12	NM_001227	CASP7	Executor and effector proteins	1.0731	*0.67144*
D01	NM_001228	CASP8	Executor and effector proteins	-1.7663	*0.006703*
D02	NM_001229	CASP9	Executor and effector proteins	-1.7186	*0.004419*
				Fold Regulation	***p-value***
Position	**Refseq**	**Symbol**	**Apoptotic pathway/category**	**DF vs UF**	***DF vs UF***
D03	NM_001242	CD27	Death receptors and ligands	-3.2806	*0.009785*
D04	NM_001250	CD40	Death receptors and ligands	-1.316	*0.325528*
D05	NM_000074	CD40LG	Death receptors and ligands	-1.9686	*0.013581*
D06	NM_001252	CD70	Death receptors and ligands	-1.658	*0.202356*
D07	NM_003879	CFLAR	Anti-apoptotic/pro-survival	-2.1141	*0.00051*
D08	NM_001279	CIDEA	Executor and effector proteins	-1.5513	*0.228807*
D09	NM_014430	CIDEB	Executor and effector proteins	-1.7336	*0.02284*
D10	NM_003805	CRADD	Pro-apoptotic	-1.0064	*0.972725*
D11	NM_018947	CYCS	Pro-apoptotic	-2.4964	*0.000313*
D12	NM_004938	DAPK1	Pro-apoptotic	-1.9165	*0.067307*

E01	NM_004401	DFFA	Executor and effector proteins	1.0199	*0.811724*
E02	NM_019887	DIABLO	Pro-apoptotic	-1.3226	*0.228869*
E03	NM_003824	FADD	Pro-apoptotic	1.0296	*0.882835*
E04	NM_000043	FAS	Death receptors and ligands	-2.3589	*0.000088*
E05	NM_000639	FASLG	Death receptors and ligands	-2.0387	*0.003289*
E06	NM_001924	GADD45A	Pro-apoptotic	1.1384	*0.534175*
E07	NM_003806	HRK	Pro-apoptotic	-1.4549	*0.155279*
E08	NM_000875	IGF1R	Anti-apoptotic/pro-survival	-1.2957	*0.163936*
E09	NM_000572	IL10	Anti-apoptotic/pro-survival	-2.0572	*0.044915*
E10	NM_000595	LTA	Death receptors and ligands	-1.0591	*0.978922*
E11	NM_002342	LTBR	Death receptors and ligands	-1.3791	*0.057066*
E12	NM_021960	MCL1	Anti-apoptotic/pro-survival	-1.5719	*0.026338*
F01	NM_004536	NAIP	Anti-apoptotic/pro-survival	-3.6072	*0.00147*
F02	NM_003998	NFKB1	Anti-apoptotic/pro-survival	-1.438	*0.027655*
F03	NM_006092	NOD1	Executor and effector proteins	-2.137	*0.000112*
F04	NM_003946	NOL3	Anti-apoptotic/pro-survival	-1.5877	*0.006106*
F05	NM_013258	PYCARD	Pro-apoptotic	2.0788	*0.006742*
F06	NM_003821	RIPK2	Pro-apoptotic	1.3458	*0.01402*
F07	NM_000594	TNF	Death receptors and ligands	-1.4549	*0.155279*
F08	NM_003844	TNFRSF10A	Death receptors and ligands	-1.7219	*0.099106*
F09	NM_003842	TNFRSF10B	Death receptors and ligands	-1.6676	*0.043374*
F10	NM_002546	TNFRSF11B	Death receptors and ligands	-1.4796	*0.208317*
F11	NM_001065	TNFRSF1A	Death receptors and ligands	-1.8542	*0.02651*
F12	NM_001066	TNFRSF1B	Death receptors and ligands	-1.1768	*0.715645*
G01	NM_014452	TNFRSF21	Death receptors and ligands	1.8737	*0.07722*
G02	NM_003790	TNFRSF25	Death receptors and ligands	-3.6224	*0.000468*
G03	NM_001561	TNFRSF9	Death receptors and ligands	-1.2813	*0.674319*
G04	NM_003810	TNFSF10	Death receptors and ligands	1.2602	*0.171339*

G05	NM_001244	TNFSF8	Death receptors and ligands	-1.5442	*0.136328*
G06	NM_000546	TP53	Pro-apoptotic	1.3765	*0.159191*
G07	NM_005426	TP53BP2	Pro-apoptotic	-1.9209	*0.005864*
G08	NM_005427	TP73	Pro-apoptotic	-1.9914	*0.068535*
				Fold Regulation	***p-value***
Position	**Refseq**	**Symbol**	**Apoptotic pathway/category**	**DF vs UF**	***DF vs UF***
G09	NM_003789	TRADD	Pro-apoptotic	-1.4995	*0.041893*
G10	NM_021138	TRAF2	Pro-apoptotic	-1.5841	*0.029047*
G11	NM_003300	TRAF3	Pro-apoptotic	-1.0815	*0.481774*
G12	NM_001167	XIAP	Anti-apoptotic/pro-survival	1.4862	*0.744222*
H01	NM_001101	ACTB	N/A	1.5942	*0.109598*
H02	NM_004048	B2M	N/A	1.4349	*0.065041*
H03	NM_002046	GAPDH	N/A	1.2743	*0.3344*
H04	**NM_000194**	**HPRT1**	**N/A**	**1**	***0***
H05	NM_001002	RPLP0	N/A	1.6461	*0.013995*

***Bold: Housekeeping gene used for quantification**